Reliability analysis for systems based on degradation rates and hard failure thresholds changing with degradation levels

Miaoxin Chang[a], Xianzhen Huang[a*,c], Frank PA Coolen[b], Tahani Coolen-Maturi[b]

[a]School of Mechanical Engineering and Automation, Northeastern University, Shenyang 110819, China

[b]Department of Mathematical Sciences, Durham University, Durham DH1 3LE, United Kingdom

[c]Key Laboratory of Vibration and Control of Aero Propulsion Systems Ministry of Education of China, Northeastern University, Shenyang, 110819, China

Abstract Degradation-shock failure processes widely exist in practice, and extensive work has been carried out to better describe such processes. In this paper, a new model is developed for reliability analysis of systems subject to dependent degradation-shock failure processes. The proposed model extends the previous work by considering the effects of the degradation levels on both the degradation rates and the hard failure thresholds. Instead of shifting with the shock levels, the degradation rates are supposed to increase with the degradation levels, and the hard failure thresholds decrease when the system deteriorates to certain levels. Then, the general reliability functions for the systems subject to multi-state degradation are provided, after deriving the reliability formulas for the systems with two-state degradation. In addition, the accuracy of the proposed methods is verified by Monte-Carlo simulation. Finally, a numerical example is presented to illustrate the validity of the presented model, and analytical results of the proposed model are compared with previous work. The results indicate that the presented method offers a more realistic system reliability evaluation.

* Corresponding Author
E-mail addresses: changmiaoxin@stumail.neu.edu.cn (M.X. Chang), xzhhuang@mail.neu.edu.cn (X.Z. Huang), frank.coolen@durham.ac.uk (F. Coolen) tahani.maturi@durham.ac.uk (T. Coolen-Maturi).

Keywords: system reliability; competing failure processes; changing failure thresholds; changing degradation rates; multiple states.

1. Introduction

As modern industrial products are increasingly reliable, the reliability analysis based on the failure data becomes more challenging, since sufficient sets of failure data are more difficult to obtain due to limited experiment budget and time [1]. Compared with the failure data obtained by destructive tests, the degradation data containing extensive reliability information could be easier to obtain by monitoring sensors. Therefore, studies on system reliability based on degradation processes have been extensively carried out [2-4].

The performance deterioration widely exists in practice. For example, the wear of mechanical products [5-6]; the corrosion of sea bridges [7-9]; and the life reduction of batteries [10]. There are commonly used degradation processes, including the general path process, the Wiener process, the Gamma process, and the Inverse Gaussian process etc. When the performance of the system deteriorates, random shocks often occur. For example, there are shocks caused by vibrations during the wear processes of mechanical systems. Besides, shocks caused by shifting voltages and currents can appear when the performance of the batteries is getting worse. The extreme shock process, δ-shock process, cumulative shock process, and m-shock process are commonly used to describe shock processes. More details about the degradation processes and shock patterns can be found in [5-6, 11-13]. Generally, a system is supposed to fail mainly due to two failure modes, one is the soft failure caused by the system degradation, and the other is the hard failure resulting from random shocks. No matter which failure occurs, it can lead the system to fail. In recent years, based on practical needs of the industry, extensive studies on competing failure processes have been carried out [15-17].

Depending on whether the degradation rates and hard failure thresholds change or not, the research on competing failure processes can be divided into three types. The first type of research mainly focuses on the reliability analysis with fixed degradation rates and fixed hard failure thresholds. Lei et al. [18] divided the shocks into three zones, and the shocks can cause the system to degrade only when their magnitudes are larger than the level of the first zone. An et al. [19] proposed a new reliability model by

considering multiple degradation processes, and six kinds of copula functions were used to describe the dependence among different degradation processes. Fan et al. [20] presented a new reliability method for the hydraulic control system based on the degradation-shock dependence, in which the arrival rate of the shock was assumed to change with the degradation level. Song et al. [21] established a reliability model for the system with multiple components and presented four different patterns based on the effects of shock magnitudes on shock damages. Song et al. [22] proposed an *s*-dependent failure model for the multi-component system. The studies above have significantly extended the work on competing failure processes. However, in the above work, degradation rates and failure thresholds are considered to be fixed, which are not appropriate for many practical cases.

The system usually deteriorates at a shifting degradation speed since the degradation rate can be affected by self-healing, degradation levels, and random shocks. Liu et al. [23] modelled the degradation rate as a variable that can decrease due to system self-healing. Bian et al. [24-25] considered the degradation rate to be composed of two parts, one is the independent degradation rate, and the other is affected by the degradation levels of other components. Similarly, Dao et al. [26] presented that the degradation levels can directly affect both the degradation states and degradation rates. Shen et al. [27] established a reliability model for a multi-component system subject to categorized shocks, and the degradation levels of the shock-sensitive components could cause degradation acceleration to other components. Dong et al. [28] analyzed the system reliability based on a binary Wiener process, and the interaction between different degradation characteristics was considered. It was assumed that, when one of the performance characteristics reached a certain degradation level, the system degenerated to the next state and the degradation rate changed. However, the studies [24-26, and 28] mainly focused on modeling multi-component or multi-characteristic systems subject to degradation processes without considering random shocks. Practically, random shocks can significantly affect the degradation rates of systems. For example, the structural deterioration of sea bridges accelerates when big shock loads occur, such as vessel collisions and earthquakes [29]. For such a scenario, Hao and Yang [29] presented a reliability model for a sea bridge system subject to shifting degradation rates and mixed shock patterns. Rafiee et al. [30] established a new reliability model with three different shock patterns, and the growth of the degradation accelerates when the shock load reaches a certain level. Gao et al. [31] modeled the

degradation as two different processes, the general path process and the Weiner process. Hao et al. [29], Rafiee et al. [30], and Gao et al. [31] considered the degradation rate of the system to change with the shock magnitude. The work above has made significant progress in modeling the competing failure process by considering the degradation rates as variables instead of constants, but the failure thresholds were assumed as fixed.

In some cases, the failure thresholds are not constants but they are changing dependently with the degradation-shock processes. Many researchers carried out the research on system reliability based on changing failure thresholds. Gao et al. [10] proposed a reliability model with abruptly changing soft failure thresholds based on the fact that the performance of the bus battery changes sharply with the temperature of different seasons. Wang et al. [32] presented a reliability model for a system experiencing intensive shocks, and the soft failure threshold was considered to change with the number of shocks. In addition to changing soft failure thresholds, some researchers focused on shifting hard failure thresholds. Dong et al. [17] considered the hard failure thresholds to change with the shock levels and analyzed the reliability of the systems based on three different shock patterns. Hao et al. [33] described the hard failure threshold as a function of the degradation level, continuously changing over time. Akiyama et al. [34] proposed a new reliability model for a bridge system by considering the shock resistance ability to change with an environmental factor, the airborne chloride. In addition to continuously changing hard failure thresholds, some researchers established reliability models based on discrete hard failure thresholds. Rafiee et al. [35] presented a new reliability model, in which, the hard failure threshold was considered to discretely change with the degradation level. Guan et al. [36] extended the work of Rafiee et al. [35] by establishing a reliability model for a multi-component system. Compared with the models based on fixed failure thresholds, the soft failure thresholds or the hard failure thresholds were considered to change with the degradation-shock levels, but the degradation rates were not considered to change as well [10, 17, and 33-36].

In short, the research on reliability analysis for competing failure processes has been extensively carried out. However, to the best of our knowledge, few studies have been carried out with the consideration of the effects of degradation levels on both degradation rates and hard failure thresholds. As the system deteriorates, the degradation of the system gets faster and its ability to resist random

shocks declines, hence both degradation rates and the hard failure thresholds should be supposed to change with the degradation levels. There are many examples of this scenario in practice. For example, as the corrosion pits of the dam or bridge develop, their structural deterioration accelerates and their ability to resist big flood peaks becomes weaker; in some areas, as the soil erosion becomes severe, the ecological environment is getting worse at a faster speed and its ability to resist intensive rainfalls declines, which may finally lead to debris flow; the crack size of the mechanical product develops faster when the degradation level is higher and the hard failure occurs more often when experiencing random shocks.

Based on the practical needs, a more realistic and practical reliability model is proposed with consideration of the dependence between the degradation level and the degradation rate, which is the difference from the previous work. In this paper, both degradation rates and hard failure thresholds changing with degradation levels are considered. Section 2 shows the motivation and commonly used assumptions, and the failure modes of the system are described in detail. The proposed model is based on the general path process and the extreme shock pattern, and the reliability analysis of other competing failure processes can be obtained by analogy. In section 3, the analytical equations for calculating the reliability of the system with two-state deterioration and multi-state deterioration are derived respectively in Section 3. In Section 4, the Monte Carlo simulation is carried out to verify the accuracy of the proposed model. Furthermore, a practical example of MEMS (Micro-Electro-Mechanical Systems) is used to illustrate and discuss the meaning and effectiveness of the presented model, then the results are compared and discussed in detail. Finally, the conclusions are summarized and future challenges are discussed in Section 5.

2. System description

2.1 Motivation and assumptions

In this paper, both the degradation rates and the hard failure thresholds are considered to change with the degradation levels of the system. There are many practical scenarios where such a situation occurs. In addition to the examples given in the introduction part, two further examples are as follows.

1) The degradation of LED lighting systems: a LED system suffers from a soft failure when the light output reduces to 70% of the initial performance. Heat management is the dominant factor that affects its degradation rates. As the chips, the package materials, and the heat sink of the LED deteriorate, the heat production increases, but the speed of heat transmission decreases, then not only the light output of the LED system reduces at a faster speed but also the hard failure is triggered more often due to random shocks caused by the vibrations of currents and voltages [40].

2) The crack growth of mechanical systems: the fatigue crack is one of the dominant failure modes of mechanical systems. As the size of the crack becomes larger, not only the growth of the crack gets faster but also the hard failure due to vibrations and random loads is triggered more often [41].

All of the assumptions made in this paper are as follows, which are commonly used in [17-18, 21-22, and 35-36].

1) The system is not repaired during the lifetime. Degradation of the system is supposed to follow a general path process, and the shock process follows the Extreme shock process. A soft failure occurs when the total degradation value exceeds the soft failure threshold, and a hard failure is triggered when the shock magnitude exceeds the hard failure threshold.

The degradation can also follow other stochastic processes, such as the Gamma process, the Inverse Gaussian process and the Wiener process, and the equations are presented in **Appendix A** [5-6, 11-13]. Besides, the shock process could be a δ-shock process or an *m*-shock process, and the calculation of the probability that the system survives from the hard failure process could be derived according to [30 and 35].

2) The hard failure thresholds D_j are supposed to be decreasing constants, and the basic parameters including the degradation rates β_j, the shock magnitudes W_i, and the shock damages Y_i are assumed to be normally distributed. The assumptions are commonly used in [18-22, and 35-36]. For example, the degradation rate of the MEMS (Micro-Electro-Mechanical System) is $\beta=2\pi rcF$, where r is the radius of the pin joint, c is the coefficient, F is the force between rubbing surfaces, c and F are constants. Considering that the parameters of the same batch of products are generally assumed to follow the normal distribution, the radius of the pin joint r is considered to be normally distributed. Hence, the degradation rates β_j are considered as normally distributed parameters. The shock magnitudes W_i, and

the shock damages Y_i are also commonly considered to follow the normal distribution [18-22, and 35-36], but the shock sizes and shock damages could be time-dependent or follow other distributions, such as the exponential distribution, the phase-type distribution and the log-normal distribution, and the calculation of reliability could be obtained according to [37-38].

2.2 Description of competing failure processes

It can be seen from **Figs. 1-2** that the system is supposed to experience both degradation and shock processes. The total degradation value $X_S(t)$ at time t is composed of two parts, that is, $X_S(t)= X(t)+ S(t)$, $X(t)$ is the continuous degradation and $S(t)$ is the abrupt degradation caused by the shocks. The system can fail due to two failure modes: 1) the system suffers from a soft failure when the total degradation value exceeds the soft failure threshold H; 2) when the system deteriorates to the jth state, the system suffers from a hard failure when the shock magnitude exceeds the hard failure threshold D_j, where, j=1, 2, …, k+1. No matter which failure mode occurs, the system is triggered to fail.

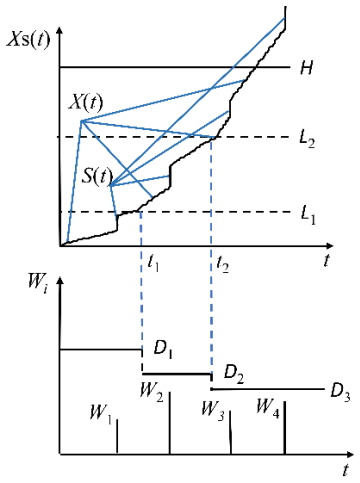

Fig. 1 System description

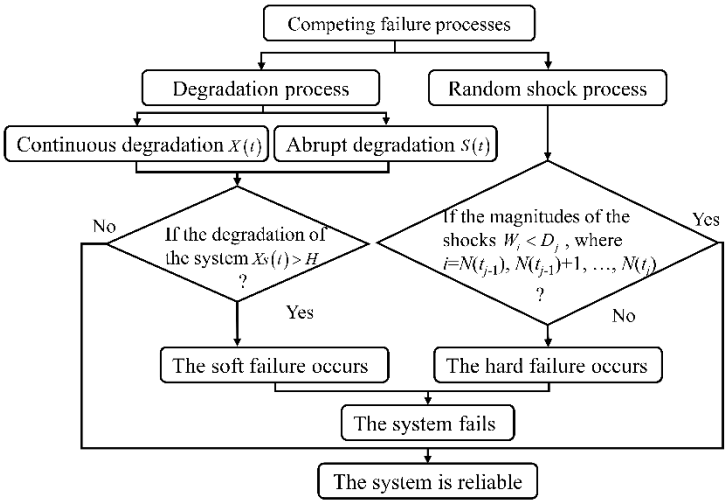

Fig. 2 The failure modes of the system

Compared with the existing literature, the novelty of this model is that both degradation rates and hard failure thresholds are considered to change with degradation levels. When the total degradation values reach L_j, the degradation rates change from β_j to β_{j+1} (j=1, 2, …, k+1), the hard failure thresholds change from D_j to D_{j+1}, and the competing failure processes are divided into k+1 states. For example, 1) when k=0, the degradation rate and the hard failure threshold of the system do not change and the system

degrades with one state; 2) when k=1, that is, β_j and D_j of the system change once at t_1 when the degradation level reaches L_1, and the competing failure processes of the system are divided into two states by t_1; 3) By analogy, when k=2, β_j and D_j of the system change twice, and the competing failure processes of the system are divided into three states by t_1 and t_2 when the degradation level reaches L_1 and L_2, respectively.

3 Reliability analysis for competing failure processes

In this section, reliability models for both the degradation process and the shock process are established. The degradation process is modeled with multiple degradation rates, which are firstly considered to change with the deterioration levels in this paper. Besides, the shock process is described with multiple failure thresholds, and the hard failure thresholds are supposed to change with the deterioration states. Then the reliability functions for the systems subject to multi-state competing failure processes are derived, after modelling the reliability for the systems deteriorating with two states.

3.1 Reliability analysis for the degradation process

The degradation rate is supposed to change with the degradation levels. When the total degradation reaches a higher level L_j, the system is supposed to deteriorate at a faster speed, that is, the degradation rate changes from β_j to β_{j+1}. The degradation of the system could also decrease due to self-healing, but this case is not included in this paper. In this section, the general reliability function for the system subject to soft failure is derived, then the reliability for other degradation processes could be obtained by analogy.

The continuous degradation value of the system with multiple degradation rates, $X(t)$, is:

$$X(t)=\varphi+\beta_1 t_1+\beta_2(t_2-t_1)+\ldots+\beta_{k+1}(t-t_k) \tag{1}$$

where, φ is the initial degradation value of the system, t_k is the time when the total degradation value reaches L_k, k=0, 1, 2, …, t_0=0, and L_0=0. The degradation rate of the jth state, β_j, follows the normal distribution $\beta_j \sim \mathcal{N}\left(\mu_{\beta_j}, \sigma_{\beta_j}^2\right)$, j=1, 2, …, k+1.

Besides the degradation process, the system is supposed to experience an extreme shock process,

which follows a Poisson process with parameter λ [39]. The total degradation damage caused by random shocks, $S(t)$, is:

$$S(t)=\begin{cases}\sum_{i=1}^{N(t)}Y_i, & (N(t)\neq 0)\\ 0, & (N(t)=0)\end{cases} \tag{2}$$

where, $N(t)$ is the number of shocks, Y_i is the abrupt degradation damage caused by the ith shock. In this paper, the degradation damage Y_i is supposed to follow the Normal distribution, $Y_i \sim \mathcal{N}\left(\mu_Y, \sigma_Y^2\right)$ as [18-21].

The total degradation value of the system, $Xs(t)$, is:

$$Xs(t)=X(t)+S(t) \tag{3}$$

If the total degradation value exceeds H, then the system experiences a soft failure. The probability that the system survives from a soft failure is:

$$\begin{aligned}P_s(t)&=\sum_{n=0}^{\infty}P\left(Xs(t)<H, N(t)=n\right)\\ &=\sum_{n=0}^{\infty}P\left(X(t)+S(t)<H\middle|N(t)=n\right)\cdot P\left(N(t)=n\right)\\ &=P\left(X(t)<H\middle|N(t)=0\right)\cdot P\left(N(t)=0\right)\\ &+\sum_{n=1}^{\infty}\int_0^H P\left(X(t)<H-u\middle|S(t)=u, N(t)=n\right)f_{S(t)}\left(u\middle|N(t)=n\right)du\cdot P\left(N(t)=n\right)\end{aligned} \tag{4}$$

where, H is the soft failure threshold, $f_{S(t)}(u|N(t)=n)$ is the PDF (Probability Density Function) of the degradation value caused by random shocks.

If Y_i and β_j are normally distributed, $f_{S(t)}(u|N(t)=n)$ and Eq. (4) can be expressed as:

$$f_{S(t)}\left(u\middle|N(t)=n\right)=\frac{1}{\sqrt{2\pi n\sigma_Y^2}}\exp\left(-\frac{(u-n\mu_Y)2}{2n\sigma_Y^2}\right), n\neq 0 \tag{5}$$

$$\begin{aligned}P_S(t)&=\sum_{n=0}^{\infty}P\left(Xs(t)<H, N(t)=n\right)\\ &=\sum_{n=0}^{\infty}P\left(Xs(t)<H\middle|N(t)=n\right)\cdot P\left(N(t)=n\right)\\ &=\sum_{n=0}^{\infty}\Phi\left(\frac{H-(\varphi+\sum_{j=1}^{k+1}\mu_{\beta_j}\left(t_j-t_{j-1}\right)+n\mu_Y)}{\sqrt{\sum_{j=1}^{k+1}\sigma_{\beta_j}^2\left(t_j-t_{j-1}\right)^2+n\sigma_Y^2}}\right)\cdot e^{-\lambda t}\frac{(\lambda t)^n}{n!}\end{aligned} \tag{6}$$

where, $\Phi(\cdot)$ is the CDF (Cumulative Distribution Function) of the standard normal random variable, t_{j-1} is the start time of the jth state, t_j is the end time of the jth state, j=1, 2, …, k+1. If j=1 and j= k+1, then t_0=0, t_{k+1}=t. λ is the arrival rate of the shock process.

When the continuous degradation process follows the Inverse Gaussian process, the Gamma process or the Wiener process, the CDF of the degradation value caused by a continuous degradation process, $P(X(t)<H-u|S(t)=u, N(t)=n)$, can be obtained according to [5, 11-13] and the derivations are presented in **Appendix A**.

3.2 Reliability analysis for the random shock process

The magnitude of the ith shock, W_i, is supposed to follow a normal distribution: $W_i \sim \mathcal{N}\left(\mu_W, \sigma_W^2\right)$.

As shown in **Fig. 1**, if the shock magnitude exceeds the hard failure thresholds D_j, then the system fails due to hard failures. When the system deteriorates, its ability to resist random shocks is getting weaker and the system is more vulnerable to fail due to random shocks. For such a scenario, a reliability model based on multiple hard failure thresholds is established. The probability of the multi-state system surviving from the hard failure is:

$$\begin{aligned} P_H(t) &= \sum_{n=0}^{\infty}\sum_{n_1=0}^{n}\sum_{n_2=0}^{n-n_1}\cdots\sum_{n_k}^{n-(n_1+\cdots+n_{k-1})} P\left\{\bigcap_{i=1}^{N(t_1)}\left(W_i<D_1\right), \bigcap_{i=N(t_1)+1}^{N(t_2)}\left(W_i<D_2\right),\cdots,\right. \\ &\quad \left.\bigcap_{i=N(t_k)+1}^{N(t)}\left(W_i<D_{k+1}\right), N(t_1)=n_1, N(t_2)=n_2,\cdots, N(t-t_k)=n-(n_1+\cdots n_k)\right\} \\ &= \sum_{n=0}^{\infty}\sum_{n_1=0}^{n}\sum_{n_2=0}^{n-n_1}\cdots\sum_{n_k=0}^{n-(n_1+\cdots+n_{k-1})} P\left(\bigcap_{i=1}^{N(t_1)}\left(W_i<D_1\right), \bigcap_{i=N(t_1)+1}^{N(t_2)}\left(W_i<D_2\right),\cdots,\right. \\ &\quad \left.\bigcap_{i=N(t_k)+1}^{N(t)}\left(W_i<D_{k+1}\right)\middle| N(t_1)=n_1, N(t_2)=n_2,\cdots, N(t-t_k)=n-(n_1+\cdots n_k)\right) \\ &\quad \cdot P\left(N(t_1)=n_1, N(t_2)=n_2,\cdots, N(t-t_k)=n-(n_1+\cdots n_k)\right) \end{aligned} \tag{7}$$

where, $N(t_j-t_{j-1})$ is the number of shocks in the jth state, D_j is the hard failure threshold of the jth state, j=1, 2, …, k+1.

The parameters W_i and Y_i are supposed to follow normal distributions, then the reliability of the hard failure process calculated by Eq. (7) can be derived as:

$$
\begin{aligned}
P_H(t) &= \sum_{n=0}^{\infty}\sum_{n_1=0}^{n}\sum_{n_2=0}^{n-n_1}\cdots\sum_{n_k=0}^{n-(n_1+\cdots+n_{k-1})}\left[\Phi\left(\frac{D_1-\mu_W}{\sigma_W}\right)\right]^{n_1}\cdot\left[\Phi\left(\frac{D_2-\mu_W}{\sigma_W}\right)\right]^{n_2}\cdots\left[\Phi\left(\frac{D_{k+1}-\mu_W}{\sigma_W}\right)\right]^{n-(n_1+\cdots n_k)} \\
&\cdot e^{\lambda t_1}\frac{(\lambda t_1)^{n_1}}{n_1!}\cdot e^{\lambda(t_2-t_1)}\frac{(\lambda(t_2-t_1))^{n_2}}{n_2!}\cdots e^{\lambda(t-t_k)}\frac{(\lambda(t-t_k))^{n-(n_1+\cdots n_k)}}{(n-(n_1+\cdots n_k))!} \\
&= \sum_{n=0}^{\infty}\sum_{n_1=0}^{n}\sum_{n_2=0}^{n-n_1}\cdots\sum_{n_k=0}^{n-(n_1+\cdots n_{k-1})}\left[\Phi\left(\frac{D_1-\mu_W}{\sigma_W}\right)\right]^{n_1}\cdot\left[\Phi\left(\frac{D_2-\mu_W}{\sigma_W}\right)\right]^{n_2}\cdots\left[\Phi\left(\frac{D_{k+1}-\mu_W}{\sigma_W}\right)\right]^{n-(n_1+\cdots n_k)} \\
&\cdot e^{\lambda t}\frac{\lambda^n(t_1)^{n_1}(t_2-t_1)^{n_2}\cdots(t_k-t_{k-1})^{n_k}(t-t_k)^{n-(n_1+\cdots n_k)}}{n_1!n_2!\cdots n_k!(n-(n_1+\cdots n_k))!}
\end{aligned}
\tag{8}
$$

3.3 Reliability analysis for systems subject to competing failure processes with two states

When k=1, the degradation rate and the hard failure threshold of the system change for one time. As shown in **Fig. 3**, the competing failure processes of the system are separated into two states by t_1. Before t_1, the degradation value is less than L_1, the degradation rate and the hard failure threshold are $\beta_1 \sim \mathcal{N}\left(\mu_{\beta_1}, \sigma_{\beta_1}^2\right)$ and D_1 respectively. If the shock magnitude exceeds D_1, then the system fails due to hard failure. The degradation rate changes to $\beta_2 \sim \mathcal{N}\left(\mu_{\beta_2}, \sigma_{\beta_2}^2\right)$ and the hard failure threshold shifts to D_2 after t_1. If the degradation value reaches H, then the soft failure occurs. If the shock magnitude exceeds D_2, then the hard failure happens. No matter which type of failure occurs, it can lead the system to fail.

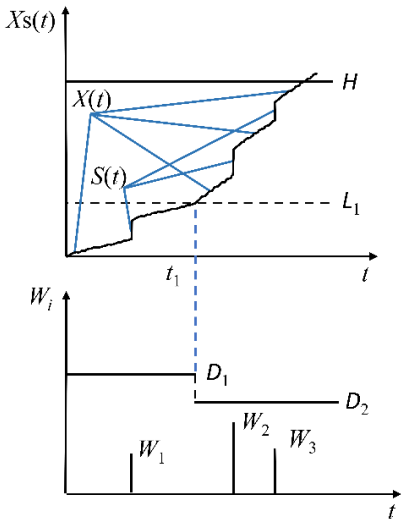

Fig. 3 System description with two states

The reliability of the system, $R_1(t)$, is calculated by two independent and mutually exclusive situations:

$$\begin{aligned} R_1(t) &= P(A_1|B_1)\cdot P(B_1) + P(A_1|B_2)\cdot P(B_2) \\ &= P(A_1B_1) + P(A_1B_2) \end{aligned} \tag{9}$$

where, A_1 is a collection of the events that the systems survive from both soft failures and hard failures; B_1 is a collection of the events that the degradation values of the systems are less than L_1 with n shocks; B_2 is a collection of the events that the degradation values of the systems are no less than L_1 with n shocks. A_1, B_1, and B_2 could be expressed as:

$$A_1 = \left(Xs(t) < H \cap \bigcap_{i=1}^{N(t_1)} (W_i < D_1) \cap \bigcap_{i=N(t_1)+1}^{N(t)} (W_i < D_2) \right)$$

$$B_1 = \bigcup_{n=0}^{\infty} \left(Xs(t) < L_1 \cap N(t) = n \right)$$

$$B_2 = \bigcup_{n=0}^{\infty} \bigcup_{n_1=0}^{n} \left(Xs(t) \geq L_1 \cap N(t_1) = n_1 \cap N(t-t_1) = n - n_1 \right)$$

1) When the total degradation value of the system is less than L_1, then the system reliability in the first case, $R_{1\_1}(t)$, is:

$$\begin{aligned} R_{1\_1}(t) &= P(A_1B_1) \\ &= \sum_{n=0}^{\infty} P\left(Xs(t) < L_1, N(t) = n, \bigcap_{i=1}^{n} (W_i < D_1) \right) \\ &= \sum_{n=0}^{\infty} P\left(X(t) + S(t) < L_1 | N(t) = n \right) \cdot P\left(N(t) = n \right) \cdot \prod_{i=1}^{n} P(W_i < D_1) \end{aligned} \tag{10}$$

2) When the degradation value of the system is equal to or greater than L_1, then the system reliability of the system in the second case, $R_{1\_2}(t)$, is:

$$\begin{aligned} R_{1\_2}(t) &= P(A_1B_2) \\ &= \sum_{n=0}^{\infty} \sum_{n_1=0}^{n} \int_0^t P\Bigg\{ Xs(t-t_1) < H - L_1, \bigcap_{i=1}^{N(t_1)} (W_i < D_1), \\ &\quad \bigcap_{i=N(t_1)+1}^{N(t)} (W_i < D_2), N(t_1) = n_1, N(t-t_1) = n - n_1 \Bigg\} f\left(t_1 | N(t_1) = n_1 \right) dt_1 \\ &= \sum_{n=0}^{\infty} \sum_{n_1=0}^{n} \int_0^t P\left(Xs(t-t_1) < H - L_1 | N(t_1) = n_1, N(t-t_1) = n - n_1 \right) \\ &\quad \cdot P(W_i < D_1)^{n_1} \cdot P(W_i < D_2)^{n-n_1} \cdot P\left(N(t_1) = n_1 \right) \cdot P\left(N(t-t_1) = n - n_1 \right) f\left(t_1 | N(t_1) = n_1 \right) dt_1 \end{aligned} \tag{11}$$

The parameters β_j, W_i, and Y_i are supposed to follow the normal distribution, then $R_1(t)$ can be derived

as follows.

$$
\begin{aligned}
R_1(t) &= R_{1\_1}(t) + R_{1\_2}(t) \\
&= \sum_{n=0}^{\infty} \Phi\left(\frac{L_1 - \left(\varphi + \mu_{\beta_1} t + n\mu_Y\right)}{\sqrt{\sigma_{\beta_1}^2 t^2 + n\sigma_Y^2}} \right) \cdot e^{-\lambda t} \cdot \frac{(\lambda t)^n}{n!} \cdot \left[\Phi\left(\frac{D_1 - \mu_W}{\sigma_W} \right) \right]^n \\
&+ \sum_{n=0}^{\infty} \sum_{n_1=0}^{n} \int_0^t \Phi\left(\frac{H - L_1 - (\mu_{\beta_2}(t-t_1) + (n-n_1)\mu_Y)}{\sqrt{\sigma_{\beta_2}^2 (t-t_1)^2 + (n-n_1)\sigma_Y^2}} \right) \cdot \left[\Phi\left(\frac{D_1 - \mu_W}{\sigma_W} \right) \right]^{n_1} \\
&\cdot \left[\Phi\left(\frac{D_2 - \mu_W}{\sigma_W} \right) \right]^{n-n_1} \cdot e^{-\lambda t_1} \cdot \frac{\left(\lambda t_1\right)^{n_1}}{n_1!} \cdot e^{-\lambda(t-t_1)} \cdot \frac{(\lambda(t-t_1))^{(n-n_1)}}{(n-n_1)!} \cdot f\left(t_1 \middle| N(t_1) = n_1\right) dt_1 \\
&= \sum_{n=0}^{\infty} \Phi\left(\frac{L_1 - \left(\varphi + \mu_{\beta_1} t + n\mu_Y\right)}{\sqrt{\sigma_{\beta_1}^2 t^2 + n\sigma_Y^2}} \right) \cdot e^{-\lambda t} \cdot \frac{(\lambda t)^n}{n!} \cdot \left[\Phi\left(\frac{D_1 - \mu_W}{\sigma_W} \right) \right]^n \\
&+ \sum_{n=0}^{\infty} \sum_{n_1=0}^{n} \int_0^t \Phi\left(\frac{H - L_1 - (\mu_{\beta_2}(t-t_1) + (n-n_1)\mu_Y)}{\sqrt{\sigma_{\beta_2}^2 (t-t_1)^2 + (n-n_1)\sigma_Y^2}} \right) \cdot \left[\Phi\left(\frac{D_1 - \mu_W}{\sigma_W} \right) \right]^{n_1} \\
&\cdot \left[\Phi\left(\frac{D_2 - \mu_W}{\sigma_W} \right) \right]^{n-n_1} \cdot e^{-\lambda t} \frac{\lambda^n \left(t_1\right)^{n_1} (t-t_1)^{(n-n_1)}}{n_1!(n-n_1)!} \cdot f\left(t_1 \middle| N(t_1) = n_1\right) dt_1
\end{aligned}
\tag{12}
$$

In Eq. (12), $f(t_1|N(t_1)=n_1)$ is the PDF of t_1, $F(t_1|N(t_1)=n_1)$ is the CDF of t_1, which can be derived as [35]:

$$
\begin{aligned}
F(t_1 | N(t_1) = n_1) &= P(T \le t_1 | N(t_1) = n_1) = P(Xs(t_1) \ge L_1 | N(t_1) = n_1) \\
&= 1 - P(Xs(t_1) < L_1 | N(t_1) = n_1) = 1 - \Phi\left(\frac{L_1 - \left(\varphi + \mu_{\beta_1} t_1 + n_1 \mu_Y\right)}{\sqrt{\sigma_{\beta_1}^2 t_1^2 + n_1 \sigma_Y^2}} \right)
\end{aligned}
\tag{13}
$$

$$
\begin{aligned}
f\left(t_1 | N(t_1) = n_1\right) &= \frac{\partial F(t_1 | N(t_1) = n_1)}{\partial t_1} \\
&= -\phi\left(\frac{L_1 - \left(\varphi + \mu_{\beta_1} t_1 + n_1 \mu_Y\right)}{\sqrt{\sigma_{\beta_1}^2 t_1^2 + n_1 \sigma_Y^2}} \right) \cdot \frac{-\mu_{\beta_1}(\sigma_{\beta_1}^2 t_1^2 + n_1 \sigma_Y^2) - \sigma_{\beta_1}^2 t_1 \left[L_1 - \left(\varphi + \mu_{\beta_1} t_1 + n_1 \mu_Y\right) \right]}{\left(\sigma_{\beta_1}^2 t_1^2 + n_1 \sigma_Y^2\right)^{\frac{3}{2}}}
\end{aligned}
\tag{14}
$$

3.4 Reliability analysis for systems subject to competing failure processes with multiple states

As shown in **Fig. 1**, when $k \ge 2$, the system degrades with multiple states. The degradation rate of the system accelerates from β_j to β_{j+1} when the degradation level of the system reaches L_j. As the system degrades, its ability to resist random shocks deteriorates from D_j to D_{j+1}, where j=1, 2, …, k+1. Then, the reliability of the system, $R_k(t)$, can be calculated as follows.

$$R_k(t)=\sum_{j=1}^{k+1}R_{k\_j}(t)=\sum_{j=1}^{k+1}P\left(A_k\left|B_j\right.\right)\cdot P\left(B_j\right)=\sum_{j=1}^{k+1}P\left(A_kB_j\right) \tag{15}$$

where,

$$A_k=\left(Xs(t)<H\cap\bigcap_{i=1}^{N(t_1)}\left(W_i<D_1\right)\cap\bigcap_{i=N(t_1)+1}^{N(t_2)}\left(W_i<D_2\right)\cap\cdots\cap\bigcap_{i=N(t_k)+1}^{N(t)}\left(W_i<D_{k+1}\right)\right)$$

$$B_j=\bigcup_{n=0}^{\infty}\bigcup_{n_1=0}^{n}\bigcup_{n_2}^{n-n_1}\cdots\bigcup_{n_{j-1}}^{n-\left(n_1+\cdots+n_{j-2}\right)}\left\{L_{j-1}\le Xs(t)<L_j\cap N\left(t_1\right)=n_1\cap N(t_2-t_1)=n_2\right.$$
$$\left.\cap N\left(t_3-t_2\right)=n_3\cdots\cap N\left(t-t_{j-1}\right)=n-\left(n_1+n_2+\cdots n_{j-1}\right)\right\}$$

n_0=0, L_0=0, and L_{k+1}=H

When the total degradation value of the system $X_S(t)\in[L_{j\text{-}1}, L_j)$, the reliability of the system $R_{k\_j}(t)$ is:

$$\begin{aligned}R_{k\_j}(t)&=P(A_kB_j)\\&=\sum_{n=0}^{\infty}\sum_{n_1=0}^{n}\sum_{n_2=0}^{n-n_1}\cdots\sum_{n_{j-1}=0}^{n-\left(n_1+n_2+\cdots+n_{j-2}\right)}\int_0^t\int_{t_1}^t\cdots\int_{t_{j-2}}^t P\left(L_{j-1}\le Xs(t)<L_j\left|\left(N(t_1)=n_1,N\left(t_2-t_1\right)=n_2,\right.\right.\right.\\&\left.\left.\left.\cdots N\left(t-t_{j-1}\right)=n-\left(n_1+n_2+\cdots+n_{j-1}\right)\right)\right)\cdot P\left(N(t_1)=n_1\right)\cdot P\left(N\left(t_2-t_1\right)=n_2\right)\\&\cdots P\left(N\left(t-t_{j-1}\right)=n-\left(n_1+n_2+\cdots+n_{j-1}\right)\right)\cdot\prod_{i=1}^{n_1}P\left(W_i<D_1\right)\prod_{i=1}^{n_2}P\left(W_i<D_2\right)\\&\cdots\prod_{i=1}^{n-\left(n_1+n_2+\cdots+n_{j-1}\right)}P\left(W_i<D_c\right)\cdot f\left(t_1\left|N(t_1)=n_1\right.\right)f\left(t_2\left|N\left(t_2\right)=n_1+n_2\right.\right)\\&\cdots f\left(t_{j-1}\left|N\left(t_{j-1}\right)=n_1+n_2+\cdots+n_{j-1}\right.\right)dt_1dt_2\cdots dt_{j-1}\end{aligned} \tag{16}$$

Especially, when j=1, $R_{k\_1}(t)$ can be calculated by Eq. (10). The parameters β_j, W_i, and Y_i are supposed to follow the normal distributions, then $R_k(t)$ can be derived as follows.

$$R_k(t)=\sum_{j=1}^{k+1}R_{k\_j}(t)$$

$$=\sum_{j=1}^{k+1}\sum_{n=0}^{\infty}\sum_{n_1=0}^{n}\sum_{n_2=0}^{n-n_1}\cdots\sum_{n_{j-1}=0}^{n-\left(n_1+\cdots n_{j-2}\right)}\int_0^t\int_{t_1}^{t}\cdots\int_{t_{j-2}}^{t}\Phi\left(\frac{L_j-L_{j-1}-\left(\mu_{\beta_j}\left(t-t_{j-1}\right)+\left(n-\sum_{a=1}^{j-1}n_a\right)\mu_Y\right)}{\sqrt{\sigma_{\beta_j}^2\left(t-t_{j-1}\right)^2+\left(n-\sum_{a=1}^{j-1}n_a\right)\sigma_Y^2}}\right)$$

$$\cdot e^{-\lambda t_1}\frac{(\lambda t_1)^{n_1}}{n_1!}\cdot e^{-\lambda(t_2-t_1)}\frac{\left(\lambda\left(t_2-t_1\right)\right)^{n_2}}{n_2!}\cdots e^{-\lambda\left(t-t_{j-1}\right)}\frac{\left(\lambda\left(t-t_{j-1}\right)\right)^{n-\sum_{a=1}^{j-1}n_a}}{\left(n-\sum_{a=1}^{j-1}n_a\right)!}\cdot\left[\Phi\left(\frac{D_1-\mu_W}{\sigma_W}\right)\right]^{n_1} \tag{17}$$

$$\cdot\left[\Phi\left(\frac{D_2-\mu_W}{\sigma_W}\right)\right]^{n_2}\cdots\left[\Phi\left(\frac{D_j-\mu_W}{\sigma_W}\right)\right]^{n-\sum_{a=1}^{j-1}n_a} f\left(t_1\middle|N(t_1)=n_1\right)f\left(t_2\middle|N\left(t_2\right)=n_1+n_2\right)$$

$$\cdots f\left(t_{j-1}\middle|N\left(t_{j-1}\right)=n_1+n_2+\cdots+n_{j-1}\right)dt_1dt_2\cdots dt_{j-1}$$

The CDF and PDF of t_j can be derived as:

$$F\left(t_{j-1}\middle|N\left(t_{j-1}\right)=n_1+n_2+\cdots+n_{j-1}\right)=P(T\le t_{j-1}\middle|N\left(t_{j-1}\right)=n_1+n_2+\cdots+n_{j-1})$$

$$=P(Xs(t_{j-1})\ge L_{j-1}\middle|N\left(t_{j-1}\right)=n_1+n_2+\cdots+n_{j-1})$$

$$=1-P(Xs(t_j)<L_{j-1}\middle|N\left(t_{j-1}\right)=n_1+n_2+\cdots+n_{j-1}) \tag{18}$$

$$=1-\Phi\left(\frac{L_{j-1}-\left(\varphi+\sum_{a=1}^{j-1}\left(\mu_{\beta_a}\left(t_a-t_{a-1}\right)+n_a\mu_Y\right)\right)}{\sqrt{\sum_{a=1}^{j-1}\left(\sigma_{\beta_{a-1}}^2\left(t_a-t_{a-1}\right)^2+n_a\sigma_Y^2\right)}}\right)$$

$$f\left(t_{j-1}\middle|N\left(t_{j-1}\right)=n_1+n_2+\cdots+n_{j-1}\right)=\frac{\partial F(t_{j-1}\middle|N\left(t_{j-1}\right)=n_1+n_2+\cdots+n_{j-1})}{\partial t_{j-1}}$$

$$=-\phi\left(\frac{L_{j-1}-\left(\varphi+\sum_{a=1}^{j-1}\left(\mu_{\beta_a}\left(t_a-t_{a-1}\right)+n_a\mu_Y\right)\right)}{\sqrt{\sum_{a=1}^{j-1}\left(\sigma_{\beta_a}^2\left(t_a-t_{a-1}\right)^2+n_a\sigma_Y^2\right)}}\right)$$

$$\cdot\left(\frac{-\mu_{\beta_{j-1}}\left(\sum_{a=1}^{j-1}\left(\sigma_{\beta_a}^2\left(t_a-t_{a-1}\right)^2+n_a\sigma_Y^2\right)\right)}{\left(\sum_{a=1}^{j-1}\left(\sigma_{\beta_a}^2\left(t_a-t_{a-1}\right)^2+n_a\sigma_Y^2\right)\right)^{\frac{3}{2}}}-\right. \tag{19}$$

$$\left.\frac{\sigma_{\beta_{j-1}}^2t_{j-1}\left(L_{j-1}-\left(\varphi+\sum_{a=1}^{j-1}\left(\mu_{\beta_a}\left(t_a-t_{a-1}\right)+n_a\mu_Y\right)\right)\right)}{\left(\sum_{a=1}^{j-1}\left(\sigma_{\beta_a}^2\left(t_a-t_{a-1}\right)^2+n_a\sigma_Y^2\right)\right)^{\frac{3}{2}}}\right)$$

where j=1,2, …, k+1.

To clarify the formula for calculating $R_k(t)$, the reliability functions for the system subject to three states competing failure processes are derived in **Appendix B**.

4 Numerical examples

A practical example of MEMS [42], carried out at Sandia National Laboratories, is widely used to illustrate degradation-shock models [18-19, 22, 30, and 35]. Hence, in this section, MEMS is also adopted to illustrate and discuss the results of the proposed model. And the Monte-Carlo simulation is applied to verify the accuracy of the presented model.

The micro-engine is supposed to fail mainly due to two competing failure processes: 1) The soft failure occurs mainly due to the degradation, which is caused by continuous wear and debris; 2) The hard failure is mainly caused by the hub fracture, which is resulting from random shocks. As the degradation of the micro-engine increases, not only its ability to resist the random shocks declines but also its growth of wear accelerates. Based on the background, a new reliability model for competing failure processes is proposed by considering the effects of degradation levels on deterioration rates and hard failure thresholds. All parameter values and the sources are provided in **Table 1**. One thing should be noted that the parameter values are obtained from difficult papers, but the set of failure data was obtained from one experiment of MEMS.

For MEMS, the wear value of the pin joint is considered as one of the performance indexes, and the degradation rate is calculated by the physical models [42-43]. For other products or systems, and the performance indexes can be selected depending on the demands of users. Then the physical models of the performance indexes can be established, and the data of the basic parameters, such as diameters, voltages, and currents, can be obtained by appropriate experiments. Finally, the proposed model can be applied to other systems with degradation-shock processes.

Table 1. Parameter values

Parameters	Values	Sources
H	0.00125μm^3	Tanner et al. [42]
L_1	0.000875μm^3	Rafiee et al. [35]
L_2	0.00095μm^3	Assumption
D_1	1.5GPa	Rafiee et al. [35]
D_2	1GPa	Assumption
D_3	0.8GPa	Assumption
φ	0	Rafiee et al. [35]
μ_{β_1}	8.4823×10^{-9}μm^3	Tanner et al. [42] and Peng et al. [43]
μ_{β_2}	10.4823×10^{-9}μm^3	Rafiee et al. [30]
μ_{β_3}	12.4823×10^{-9}μm^3	Rafiee et al. [30]
σ_{β_1}	6.0016×10^{-10}μm^3	Tanner et al. [42] and Peng et al. [43]
σ_{β_2}	8.0016×10^{-10}μm^3	Assumptions
σ_{β_3}	10.0016×10^{-10}μm^3	Assumptions
μ_Y	1.2×10^{-4}μm^3	An et al. [19]
σ_Y	4×10^{-5}μm^3	An et al. [19]
μ_W	1.2GPa	An et al. [19]
σ_W	0.4GPa	An et al. [19]
λ	5×10^{-5}/revolutions	Rafiee et al. [35]

4.1 Reliability analysis for the system by considering both degradation rates and hard failure thresholds shifting with degradation levels

To verify the accuracy of the newly proposed model, four groups of $R_1(t)$ and $F(t_1|N(t_1)=n_1)$ calculated by Eqs. (9-14) with different L_1 are checked by Monte-Carlo simulation. As shown in **Table 2** and **Fig. 4**, the reliabilities and the confidence intervals of parameters are calculated at a 95% confidence level

based on sample sizes of 10,000. It can be seen from **Figs. 4-6** that the theoretical results are very consistent with the simulation results. To get $F(t_1|N(t_1)=n_1)$, the parameter n_1 needs to be given firstly according to Eq. (13). In **Fig. 6**, n_1 is 3, but n_1 is a variable that can be any value in the range of Eq. (12), that is, $n_1 \in [0, n]$.

Table 2. Confidence intervals of parameters

Parameters	95% Confidence intervals	Parameters	95% Confidence intervals
μ_{β_1}	$(8.4779\times10^{-9}, 8.5018\times10^{-9})\mu m^3/r$	μ_Y	$(1.1938\times10^{-4}, 1.2096\times10^{-4})\mu m^3$
μ_{β_2}	$(10.475\times10^{-9}, 10.506\times10^{-9})\mu m^3/r$	σ_Y	$(3.9814\times10^{-5}, 4.0933\times10^{-5})\mu m^3$
μ_{β_3}	$(12.476\times10^{-9}, 12.516\times10^{-9})\mu m^3/r$	μ_W	(1.1963, 1.2120)GPa
σ_{β_1}	$(6.0088\times10^{-10}, 6.1778\times10^{-10})\mu m^3/r$	σ_W	(0.3941, 0.4052)GPa
σ_{β_2}	$(7.7970\times10^{-10}, 8.0161\times10^{-10})\mu m^3/r$	λ	$(4.9663\times10^{-5}, 5.033\times10^{-5})/r$
σ_{β_3}	$(9.9310\times10^{-10}, 1.0210\times10^{-10})\mu m^3/r$		

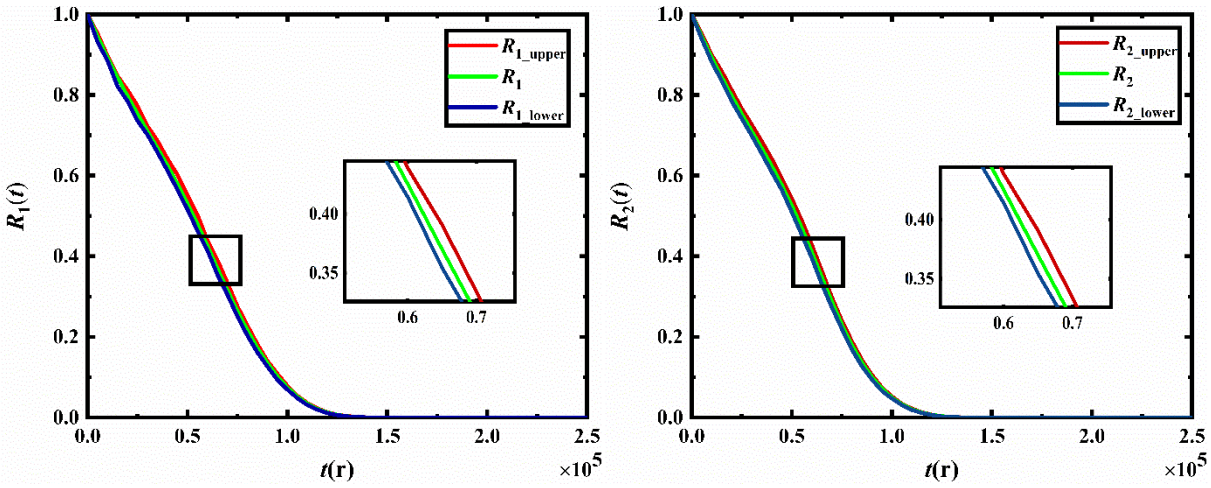

Fig. 4 The reliability curves at the 95% confidence level

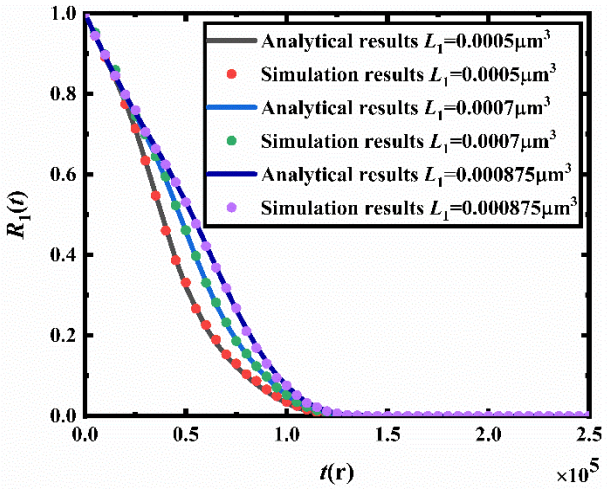

Fig. 5 The comparison of simulation and theoretical results of $R_1(t)$

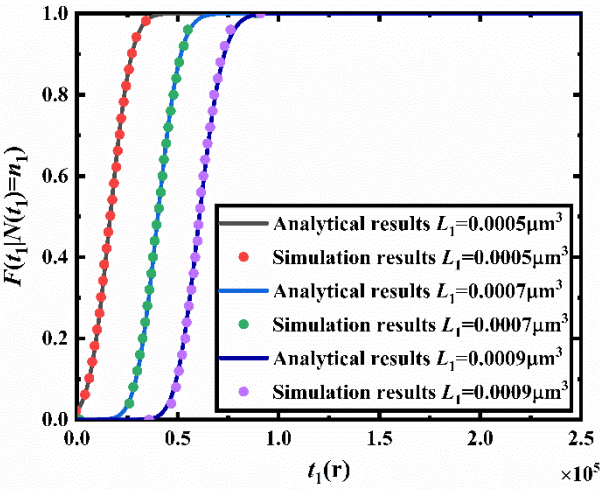

Fig. 6 The comparison of simulation and theoretical results of $F(t_1|N(t_1)=n_1)$

It can be seen from **Fig. 7** and **Fig. 8** that the simulation results are in great agreement with the theoretical ones. The analytical results of $R_2(t)$ and $F(t_2|N(t_2)=n_1+n_2)$ are calculated by Eqs. (B.1-B.8) in **Appendix B**. In **Fig. 8**, t_1 is 20,000r, n_1 is 0, and n_2 is 2. But t_1, n_1 and n_2 are variables which can be any value in the range of Eq. (B.4), that is, $t_1 \in [0, t]$, $n_1 \in [0, n]$, $n_2 \in [0, n\text{-}n_1]$.

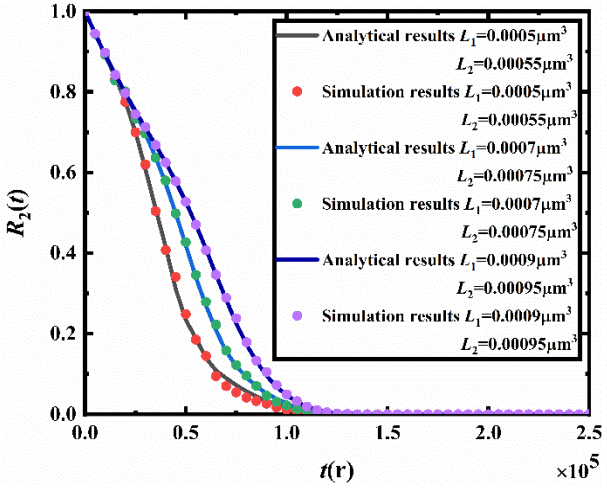

Fig. 7 The comparison of the simulation and theoretical results of $R_2(t)$

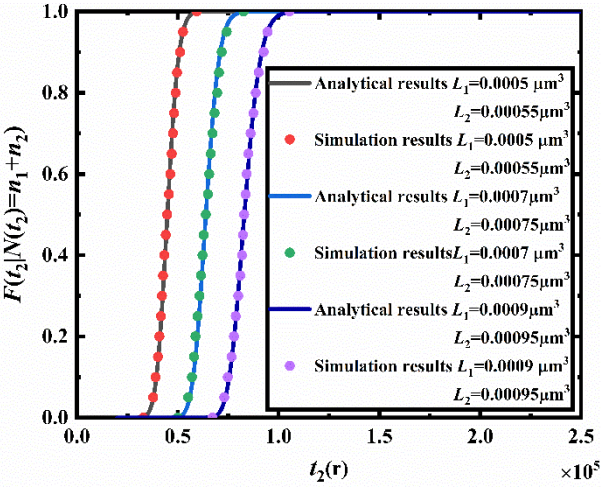

Fig. 8 The comparison of the simulation and theoretical results of $F(t_2|N(t_2)=n_1+n_2)$

The flow charts of the simulations can be seen in **Appendix C**. The simulation procedure for competing failure processes with $k \geq 2$ is similar to that with $k=1$, hence it is omitted. The simulation procedure for $R_{1\_2}(t)$ is complicated, hence it is divided into two parts, $R_{1\_21}(t)$ and $R_{1\_22}(t)$, where $R_{1\_21}(t)$ is the reliability of the system when $Xs(t) \geq L_1$ and $N(t)=0$, and $R_{1\_22}(t)$ is the reliability of the system when

$Xs(t) \geq L_1$ and $N(t) \neq 0$. Instead of sampling 10,000 times in the beginning, sampling t_1 and the number of shocks 100 times separately can help to reduce the running time from 5-6 hours to 6-7 minutes without affecting the simulation accuracy. The step size of t is: t=5,000r:5,000r:250,000r, it can also be smaller, but then the calculation time gets longer. t is set to start at 5,000r instead of zero, because there is a singular point for $R_k(t)$ when both t and n are zero, and the reliability is commonly considered to be one at the start. The shock process follows the Poisson process, which means that the biggest number of shocks is about $\lambda \times t = 5 \times 10^{-5}/\mathrm{r} \times 2.5 \times 10^5 \mathrm{r} = 12.5$, leading to the conclusion that 30 is an adequate number of shocks to ensure the accuracy of the simulation results. And the simulation of $F(t_1|N(t_1)=n_1)$ can be easily obtained by the reverse Monte-Carlo method.

As shown in **Fig. 9**, the green line is the reliability calculated by An et al. [19] with W_L=0. (An et al. [19] considered that only when the magnitude of the shock was larger than a certain level W_L, the shock could cause a degradation increment to the system. To simplify the proposed model, this assumption is not considered in this paper, that is, W_L=0.) The blue line represents the reliability calculated by Rafiee et al. [35]. The red line and the black line are the reliability curves calculated by the proposed method, which are lower than the reliability results calculated by the existing literature. Because the green line is calculated based on a fixed failure threshold, the blue line is calculated based on shifting hard failure thresholds and a fixed degradation rate. However, besides the hard failure thresholds, the degradation rates could also directly be affected by the degradation levels. For example, as the micro-engine wears, it becomes more vulnerable to random shocks and the growth of degradation becomes much faster. Therefore, the new method is proposed by considering both degradation rates and hard failure thresholds shifting with the degradation levels, and the results are lower than those calculated by the existing methods [19 and 35], which indicates that the proposed reliability model is more realistic and accurate.

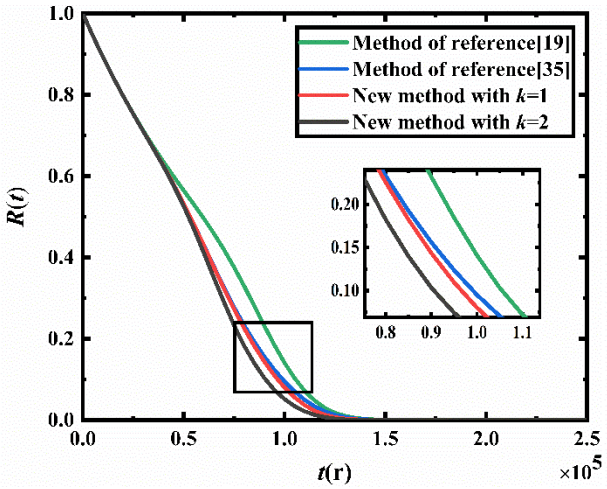

Fig. 9 The comparison of the reliability evaluations of the new and previous models

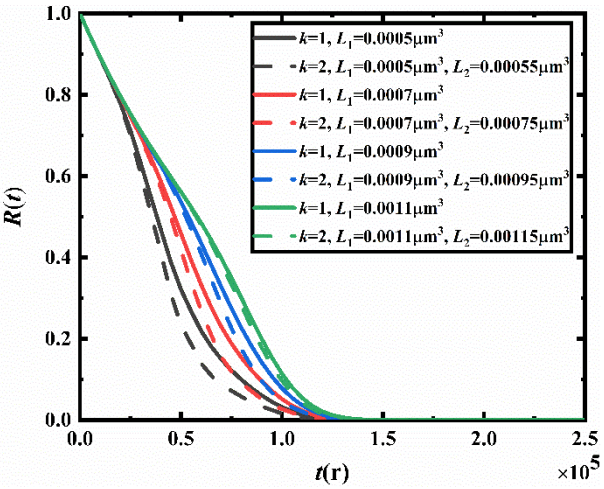

Fig. 10 The comparison of the reliability with k=1 and k=2

As shown in **Fig. 10**, the differences among the reliability results of the systems with different k and L_k are not obvious at the beginning. This is due to the fact that in the initial state the growth of wear does not accelerate and the number of shocks is close to zero. Then, the differences among the reliability curves with different k become more obvious, especially when L_1 and L_2 are lower. Because after the degradation values reach L_1 and L_2, not only the growth of degradation gets faster but also its ability to resist random shocks gets weaker. When the L_1 and L_2 are smaller, the degradation acceleration and resistance reduction start earlier. Hence, the difference between the dark lines is the biggest among the four groups. It can be seen from **Fig. 10** that the smaller L_k is, the bigger the difference between the system reliabilities with k=1 and k=2 becomes, which indicates that the reliability can be evaluated more practically and accurately if the states of the system are divided more rationally and finely according to the degradation levels.

4.2 Sensitivity analysis for the system subject to both degradation rates and hard failure thresholds shifting with degradation levels

As shown in **Figs. 11-12** that the effects of L_1 and L_2 on the system reliability are quite obvious. The curves shift to the left when the values of L_1 and L_2 become lower and the reliabilities of the systems decrease faster after the degradation levels reach L_1 and L_2. It can be explained by the fact that as the micro-engine degrades, the growth of wear gets faster and the probability of hub fracture becomes higher,

then the system becomes more easily to fail due to both the soft failure and the hard failure.

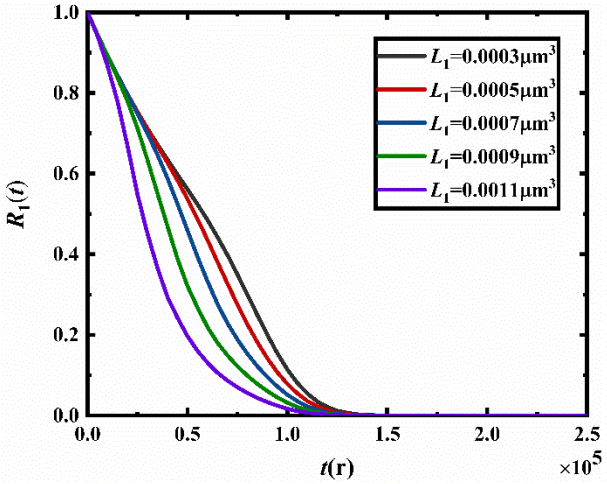

Fig. 11 The sensitivity analysis of reliability on L_1 with k=1

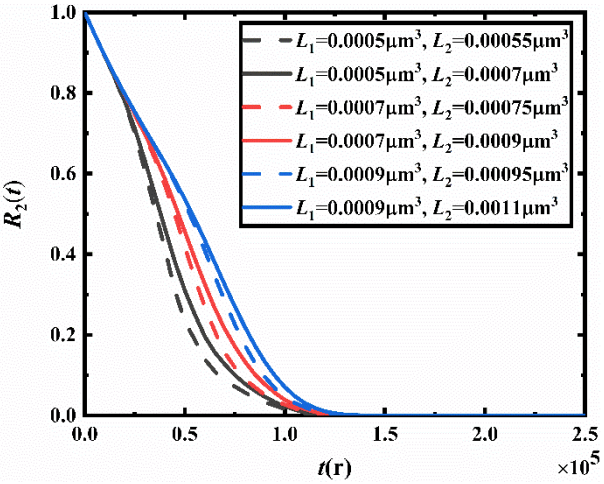

Fig. 12 The sensitivity analysis of reliability on L_1 and L_2 with k=2

As shown in **Figs. 13-14**，if the D_j (j=1, 2, …, k+1) gets smaller, the reliability curves shift to the left. It can be explained by the fact that D_j represents the system resistance to the random shocks, if the ability of the system to survive from the shocks declines, then the system becomes more easily to fail due to the hard failure. In **Fig. 13**, it can be seen that the difference between the dotted line and the dashed line becomes less obvious when L_1 changes from 0.0007μm^3 to 0.0004μm^3, while the difference between the dashed line and the solid line gets more noticeable. This is because when L_1 gets smaller, the duration of the first state is shorter while the second state lasts longer, then the effects of D_1 and D_2 become stronger and lighter respectively. Accordingly, the similar conclusion can be obtained from **Fig. 14** regarding the changes in L_1, L_2, D_2 and D_3. Compared to **Fig. 13**, the red lines and the blue lines in **Fig. 14** are separated much earlier, because the hard failure thresholds of the red lines in **Fig. 14** decrease earlier when the total degradation value reaches 0.0002μm^3 instead of 0.0004μm^3 in **Fig. 13**.

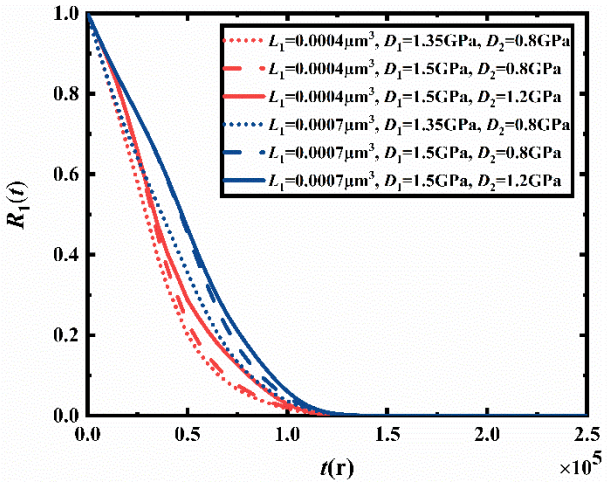

Fig. 13 Sensitivity analysis of reliability on D_1 and D_2 with k=1

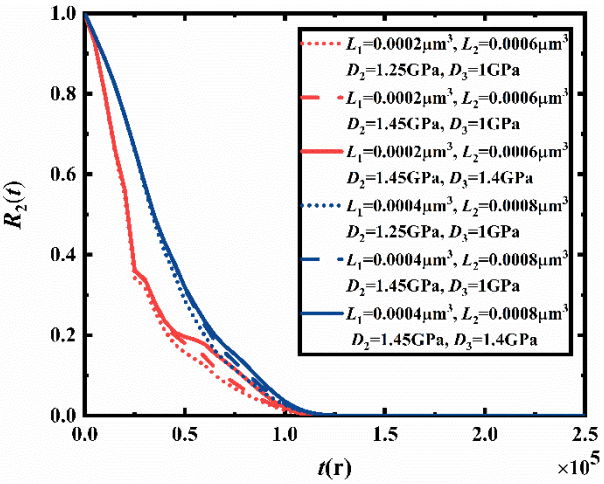

Fig. 14 Sensitivity analysis of reliability on D_2 and D_3 with k=2

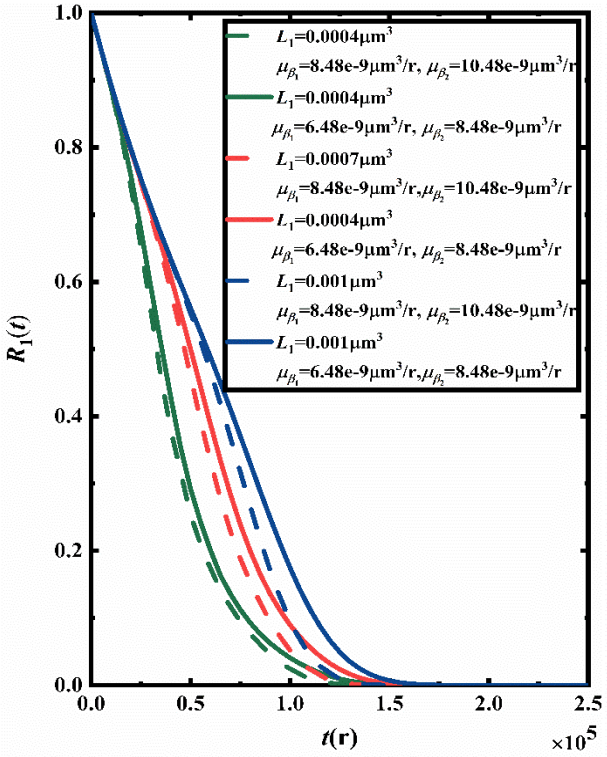

Fig. 15 Sensitivity analysis of reliability on μ_{β_1} and μ_{β_2} with k=1

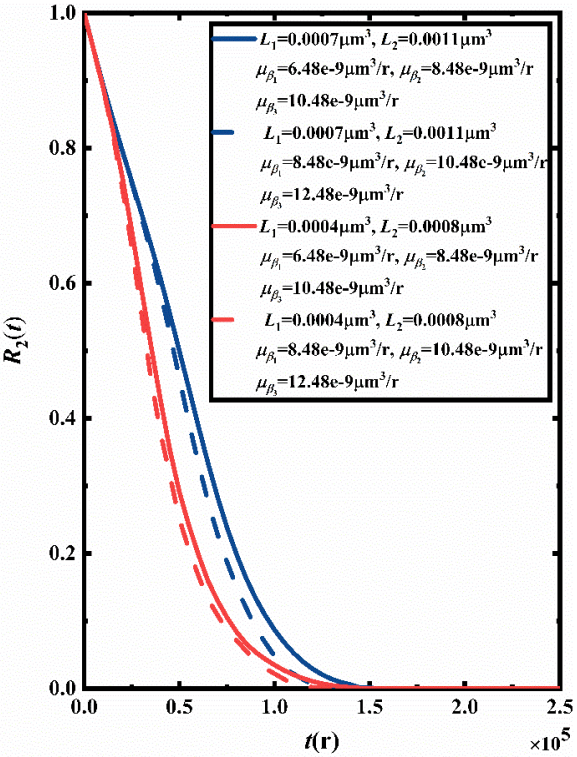

Fig. 16 Sensitivity analysis of reliability on μ_{β_1}, μ_{β_2}, and μ_{β_3} with k=2

As shown in **Figs. 15-16**, compared to D_j (j=1, 2, …, k+1), the reliability of the system becomes less sensitive to μ_{β_j}, but the effects of μ_{β_j} are still obvious. When the values of μ_{β_j} are higher, then the reliability curves shift to the left. It can be explained by the fact that μ_{β_j} represents the degradation

rates of the system, the higher the value of μ_{β_j} is, the faster the system degrades, then the probability of the system suffering from soft failure becomes greater.

As shown in **Fig. 15**, the difference between the solid lines and the dashed lines becomes increasingly obvious when L_1 is larger. This is because the reliability of the first state, that is, $R_{1\_1}(t)$, contributes to the system reliability more than $R_{1\_2}(t)$, which can be seen from **Fig. 17 (a-b)**. The values of $R_{1\_2}(t)$ are much lower than $R_{1\_1}(t)$, such as the values of the reliabilities marked as red squares in **Fig. 17 (a-b)**. Hence, the difference between the solid lines and the dashed lines in **Fig. 15** is increasingly larger because the first state lasts longer when L_1 is bigger. Similar results can be obtained from **Fig. 16** and **Fig. 17 (c-d)**.

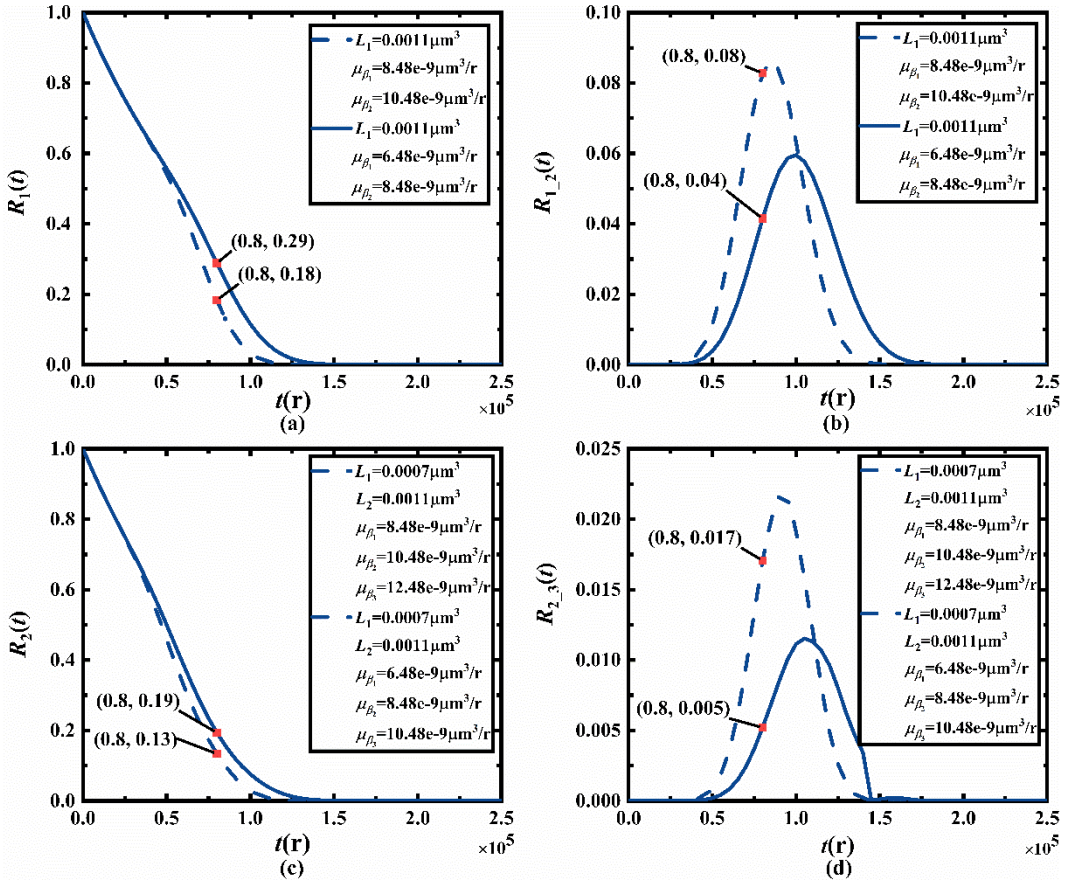

Fig. 17 Sensitivity analysis of reliability on μ_{β_j}

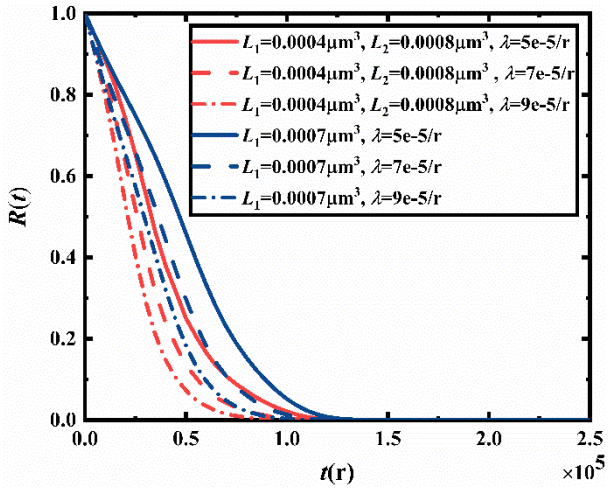

Fig. 18 Sensitivity analysis of reliability on λ

Fig. 18 shows the sensitivity of the reliability on the parameter λ, the curves shift to the left as the value of λ increases. It can be explained by the fact that the system is more vulnerable to hard failure when more random shocks occur. As shown in **Fig. 18**, initially, the differences among the red lines or the blue lines are not very big, but after 10^4 revolutions, the change of parameter λ affects the reliability in a more obvious way. It is because at the beginning, the number of shocks is close to zero and the system degrades mainly due to continuous degradation. As the time increasing, more random shocks occur, the degradation caused by random shocks becomes larger and the contribution of the hard failure is greater, then the effect of the shock arrival rate on the system reliability is increasingly obvious.

5. Conclusion

After the crack size becomes bigger, not only the crack growth of the micro-engine system accelerates but also the system becomes more likely to break down when suffering from random shocks. However, in most previous researches, the degradation rates and the hard failure thresholds are considered to change with the shock magnitudes. Motivated by the practical needs, a new model is established, where both the degradation rates and hard failure thresholds are considered to change with the degradation levels. Moreover, the analytical reliability functions for the systems subject to multi-states degradation-shock processes are derived, after analyzing the reliability for the systems with two states competing failure processes. Furthermore, a numerical example of the micro-engine and Monte-Carlo simulation are applied to illustrate and verify the proposed model.

Considering the effects of degradation levels on degradation rates and hard failure thresholds offers a more practical evaluation of the system reliability. The established model is based on the general path process and extreme shock pattern, and it can be applied to various kinds of systems or products subject to different degradation processes and shock patterns, such as the Wiener process, the Gamma process, the Inverse Gaussian process, the running shock pattern, and the δ-shock pattern. For future work, more complicated systems are worthy to focus on, such as systems composed of multiple components and systems suffering from mixed degradation processes and shock patterns. Besides, the shock size and damage are supposed to be normally distributed, the variability of the shock size and the shock damage is neglected. In future work, the time-dependent shock size and shock damage should be considered. For example, the parameters can also be functions of time t or follow other distributions, such as the Weibull distribution, the Gamma distribution, and the Phase-type distribution. In addition to modeling the system reliability, the corresponding maintenance strategies are worthy to figure out.

Acknowledgments

The work was supported by the National Natural Science Foundation of China [grant numbers 51975110]; Liaoning Revitalization Talents program [grant numbers XLYC1907171]; and Fundamental Research Funds for the Central Universities [grant numbers N2003005].

Appendix A

When the continuous degradation process follows a Wiener process, $X(t)=\beta t+\sigma B(t)$, where β represents the drift parameter, σ represents the diffusion parameter, and $B(t)$ represents a standard Brown motion process. Then, the probability that the system survives from the continuous degradation process, $P(X(t)<H-u|S(t)=u,N(t)=n)$, can be obtained according to [5].

$$P\left(X\left(t\right)<H-u\middle|S\left(t\right)=u,N\left(t\right)=n\right)=\Phi\left(\frac{H-u-\beta t}{\sigma\sqrt{t}}\right)-\exp\left(-\frac{2\beta\left(H-u\right)}{\sigma^{2}}\right)\Phi\left(-\frac{H-u+\beta t}{\sigma\sqrt{t}}\right) \quad \text{(A.1)}$$

where $\Phi(\cdot)$ is the CDF of the standard normal random variable.

When the continuous degradation process follows an Inverse Gaussian process, $X(t)\sim IG(\mu,\theta)$, where

$X(t)>0$, $\mu>0$, $\theta>0$, μ is the mean, and θ is the shape parameter. Then, the probability that the system survives from the continuous degradation process, $P(X(t)<H-u|S(t)=u,N(t)=n)$, can be obtained according to [11].

$$P\left(X(t)<H-u\middle|S(t)=u,N(t)=n\right)=\Phi\left(\sqrt{\frac{\theta}{H-u}}\left(\frac{H-u}{\mu}-1\right)\right)+\exp\left(\frac{2\theta}{\mu}\right)\Phi\left(-\sqrt{\frac{\theta}{H-u}}\left(\frac{H-u}{\mu}+1\right)\right) \tag{A.2}$$

When the continuous degradation follows a Gamma process, $X(t)\sim Ga(\omega,\eta)$, where, $\omega>0$, $\eta>0$, ω is the shape parameter, and η is the scale parameter. Then, the probability that the system survives from the continuous degradation process, $P(X(t)<H-u|S(t)=u,N(t)=n)$, can be obtained according to [12-13].

$$P\left(X(t)<H-u\middle|S(t)=u,N(t)=n\right)=\int_0^{H-u}\frac{\eta^{\omega}}{\Gamma(\omega)}z^{\omega-1}\exp(-\eta z)dz=1-\frac{\Gamma\left(\omega,\eta(H-u)\right)}{\Gamma(\omega)} \tag{A.3}$$

where, $\Gamma(\cdot)$ is the gamma function, $\Gamma(\omega)=\int_0^{\infty}t^{\omega-1}e^{-t}dt$, and $\Gamma\left(\omega,\eta(H-u)\right)=\int_{\eta(H-u)}^{\infty}t^{\omega-1}e^{-t}dt$.

Appendix B

To clarify the formula for calculating $R_k(t)$, the reliability functions for the system subject to three states are derived as follows.

$$R_2(t)=\sum_{j=1}^{3}R_{2\_j}(t)=\sum_{j=1}^{3}P\left(A_2\middle|B_j\right)P\left(B_j\right)=\sum_{j=1}^{3}P\left(A_2B_j\right) \tag{B.1}$$

where,

$$A_2=\left(Xs(t)<H\cap\bigcap_{i=1}^{N(t_1)}(W_i<D_1)\cap\bigcap_{i=N(t_1)+1}^{N(t_2)}(W_i<D_2)\cap\bigcap_{i=N(t_2)+1}^{N(t)}(W_i<D_3)\right)$$

$$B_j=\bigcup_{n=0}^{\infty}\bigcup_{n_1=0}^{n}\bigcup_{n_2=0}^{n-n_1}\cdots\bigcup_{n_{j-1}}^{n-(n_1+\cdots+n_{j-2})}\left\{L_{j-1}\le Xs(t)<L_j\cap N(t_1)=n_1\cap N(t_2-t_1)=n_2\cap\cdots\cap N\left(t-t_{j-1}\right)=n-\left(n_1+n_2+\cdots n_{j-1}\right)\right\}$$

j=1, 2, 3, n_0=0, L_0=0, and L_3=H

Especially, when j=1, the system reliability of the first case $R_{2\_1}(t)$, can be calculated by Eq. (10).

1) When the total degradation value of the system is between L_1 and L_2, then the system reliability in

the second case, $R_{2\_2}(t)$, is:

$$
\begin{aligned}
&R_{2\_2}(t) = P(A_2 B_2) \\
&= \sum_{n=0}^{\infty} \sum_{n_1=0}^{n} \int_0^t P\Big\{ L_1 \le Xs(t) < L_2, \bigcap_{i=1}^{N(t_1)} (W_i < D_1), \bigcap_{i=N(t_1)+1}^{N(t)} (W_i < D_2), \\
&N(t_1) = n_1, N(t - t_1) = n - n_1 \Big\} f\left(t_1 \middle| N(t_1) = n_1\right) dt_1 \qquad \text{(B.2)} \\
&= \sum_{n=0}^{\infty} \sum_{n_1=0}^{n} \int_0^t P\Big(Xs(t - t_1) < L_2 - L_1 \Big| \left(N(t_1) = n_1, N(t - t_1) = n - n_1 \right) \Big) \cdot P(W_i < D_1)^{n_1} \cdot P(W_i < D_2)^{n - n_1} \\
&\cdot P\left(N(t_1) = n_1\right) \cdot P\left(N(t - t_2) = n - n_1\right) f\left(t_1 \middle| N(t_1) = n_1\right) dt_1
\end{aligned}
$$

2) When the degradation value of the system is between L_2 and H, then the reliability of the system in the third case, $R_{2\_3}(t)$, is:

$$
\begin{aligned}
&R_{2\_3}(t) = P(A_2 | B_3) \cdot P(B_3) \\
&= \sum_{n=0}^{\infty} \sum_{n_1=0}^{n} \sum_{n_2=0}^{n-n_1} \int_0^t \int_{t_1}^t P\Bigg\{ L_2 \le Xs(t) < H, \bigcap_{i=1}^{N(t_1)} (W_i < D_1), \bigcap_{i=N(t_1)+1}^{N(t_2)} (W_i < D_2), \\
&\bigcap_{i=N(t_2)+1}^{N(t)} (W_i < D_3), N(t_1) = n_1, N(t_2 - t_1) = n_2, N(t - t_2) = n - n_1 - n_2 \Bigg\} \\
&\cdot f\left(t_1 \middle| N(t_1) = n_1\right) f\left(t_2 \middle| N(t_2) = n_1 + n_2\right) dt_1 dt_2 \qquad \text{(B.3)} \\
&= \sum_{n=1}^{\infty} \sum_{n_1=0}^{n} \sum_{n_2=0}^{n-n_1} \int_0^t \int_{t_1}^t P\Big(Xs(t - t_2) < H - L_2 \Big| \left(N(t_1) = n_1, N(t_2 - t_1) = n_2, N(t - t_2) = n - n_1 - n_2 \right) \Big) \\
&\cdot P(W_i < D_1)^{n_1} \cdot P(W_i < D_2)^{n_2} \cdot P(W_i < D_3)^{n - n_1 - n_2} \\
&\cdot P\left(N(t_1) = n_1\right) \cdot P\left(N(t_2 - t_1) = n_2\right) \cdot P\left(N(t - t_2) = n - n_1 - n_2\right) \\
&f\left(t_1 \middle| N(t_1) = n_1\right) f\left(t_2 \middle| N(t_2) = n_1 + n_2\right) dt_1 dt_2
\end{aligned}
$$

Then the reliability of the system calculated by Eq. (B.1) can be derived as follows.

$$
\begin{aligned}
R_2(t) &= \sum_{j=1}^{3} R_{2\_j}(t) \\
&= \sum_{n=0}^{\infty} \Phi\left(\frac{L_1 - \left(\varphi + \mu_{\beta_1} t + n\mu_Y\right)}{\sqrt{\sigma_{\beta_1}^2 t^2 + n\sigma_Y^2}} \right) \cdot e^{-\lambda t} \cdot \frac{(\lambda t)^n}{n!} \cdot \left[\Phi\left(\frac{D_1 - \mu_W}{\sigma_W} \right) \right]^n \\
&+ \sum_{n=0}^{\infty} \sum_{n_1=0}^{n} \int_0^t \Phi\left(\frac{L_2 - L_1 - (\mu_{\beta_2}(t-t_1) + (n-n_1)\mu_Y)}{\sqrt{\sigma_{\beta_2}^2 (t-t_1)^2 + (n-n_1)\sigma_Y^2}} \right) \cdot \left[\Phi\left(\frac{D_1 - \mu_W}{\sigma_W} \right) \right]^{n_1} \cdot \left[\Phi\left(\frac{D_2 - \mu_W}{\sigma_W} \right) \right]^{n-n_1} \\
&\cdot e^{-\lambda t_1} \cdot \frac{(\lambda t_1)^{n_1}}{n_1!} \cdot e^{-\lambda(t-t_1)} \cdot \frac{(\lambda(t-t_1))^{(n-n_1)}}{(n-n_1)!} \cdot f\left(t_1 \middle| N(t_1) = n_1\right) dt_1 \qquad \text{(B.4)} \\
&+ \sum_{n=0}^{\infty} \sum_{n_1=0}^{n} \sum_{n_2=0}^{n-n_1} \int_0^t \int_{t_1}^t \Phi\left(\frac{H - L_2 - (\mu_{\beta_3}(t-t_2) + (n-n_1)\mu_Y)}{\sqrt{\sigma_{\beta_3}^2 (t-t_2)^2 + (n-n_1)\sigma_Y^2}} \right) \cdot \left[\Phi\left(\frac{D_1 - \mu_W}{\sigma_W} \right) \right]^{n_1} \\
&\cdot \left[\Phi\left(\frac{D_2 - \mu_W}{\sigma_W} \right) \right]^{n_2} \cdot \left[\Phi\left(\frac{D_3 - \mu_W}{\sigma_W} \right) \right]^{n-n_1-n_2} e^{-\lambda t_1} \frac{(\lambda t_1)^{n_1}}{n_1!} \cdot e^{-\lambda(t_2-t_1)} \frac{\left(\lambda(t_2-t_1)\right)^{n_2}}{n_2!} \\
&\cdot e^{-\lambda(t-t_2)} \frac{\left(\lambda(t-t_2)\right)^{n-n_1-n_2}}{(n-n_1-n_2)!} \cdot f\left(t_1 \middle| N(t_1) = n_1\right) f\left(t_2 \middle| N(t_2) = n_1 + n_2\right) dt_1 dt_2
\end{aligned}
$$

where:

$$
\begin{aligned}
F(t_1 | N(t_1) = n_1) &= P(T \le t_1 | N(t_1) = n_1) = P(Xs(t_1) \ge L_1 | N(t_1) = n_1) \\
&= 1 - P(Xs(t_1) < L_1 | N(t_1) = n_1) = 1 - \Phi\left(\frac{L_1 - \left(\varphi + \mu_{\beta_1} t_1 + n_1 \mu_Y\right)}{\sqrt{\sigma_{\beta_1}^2 t_1^2 + n_1 \sigma_Y^2}} \right)
\end{aligned} \qquad \text{(B.5)}
$$

$$
\begin{aligned}
f\left(t_1 | N(t_1) = n_1\right) &= \frac{\partial F(t_1 | N(t_1) = n_1)}{\partial t_1} \\
&= -\phi\left(\frac{L_1 - \left(\varphi + \mu_{\beta_1} t_1 + n_1 \mu_Y\right)}{\sqrt{\sigma_{\beta_1}^2 t_1^2 + n_1 \sigma_Y^2}} \right) \cdot \frac{-\mu_{\beta_1}(\sigma_{\beta_1}^2 t_1^2 + n_1 \sigma_Y^2) - \sigma_{\beta_1}^2 t_1 \left[L_1 - \left(\varphi + \mu_{\beta_1} t_1 + n_1 \mu_Y\right) \right]}{\left(\sigma_{\beta_1}^2 t_1^2 + n_1 \sigma_Y^2\right)^{\frac{3}{2}}}
\end{aligned} \qquad \text{(B.6)}
$$

$$
\begin{aligned}
F\left(t_2 | N(t_2) = n_1 + n_2\right) &= P(T \le t_2 | N(t_2) = n_1 + n_2) = P(Xs(t_2) \ge L_2 | N(t_2) = n_1 + n_2) \\
&= 1 - P(Xs(t_2) < L_2 | N(t_2) = n_1 + n_2) \\
&= 1 - \Phi\left(\frac{L_2 - \left(\varphi + \mu_{\beta_1} t_1 + \mu_{\beta_2}(t_2 - t_1) + (n_1 + n_2)\mu_Y\right)}{\sqrt{\sigma_{\beta_1}^2 t_1^2 + \sigma_{\beta_2}^2 (t_2 - t_1)^2 + (n_1 + n_2)\sigma_Y^2}} \right)
\end{aligned} \qquad \text{(B.7)}
$$

$$
\begin{aligned}
f\left(t_2 | N(t_2) = n_1 + n_2\right) &= \frac{\partial F(t_2 | N(t_2) = n_1 + n_2)}{\partial t_2} = -\phi\left(\frac{L_2 - \left(\varphi + \mu_{\beta_1} t_1 + \mu_{\beta_2}(t_2 - t_1) + (n_1 + n_2)\mu_Y\right)}{\sqrt{\sigma_{\beta_1}^2 t_1^2 + \sigma_{\beta_2}^2 (t_2 - t_1)^2 + (n_1 + n_2)\sigma_Y^2}} \right) \\
&\cdot \frac{-\mu_{\beta_2}\left(\sigma_{\beta_1}^2 t_1^2 + \sigma_{\beta_2}^2 (t_2 - t_1)^2 + (n_1 + n_2)\sigma_Y^2\right) - \sigma_{\beta_2}^2 (t_2 - t_1)\left[L_2 - \left(\varphi + \mu_{\beta_1} t_1 + \mu_{\beta_2}(t_2 - t_1) + (n_1 + n_2)\mu_Y\right) \right]}{\left(\sigma_{\beta_1}^2 t_1^2 + \sigma_{\beta_2}^2 (t_2 - t_1)^2 + (n_1 + n_2)\sigma_Y^2\right)^{\frac{3}{2}}}
\end{aligned} \qquad \text{(B.8)}
$$

Appendix C

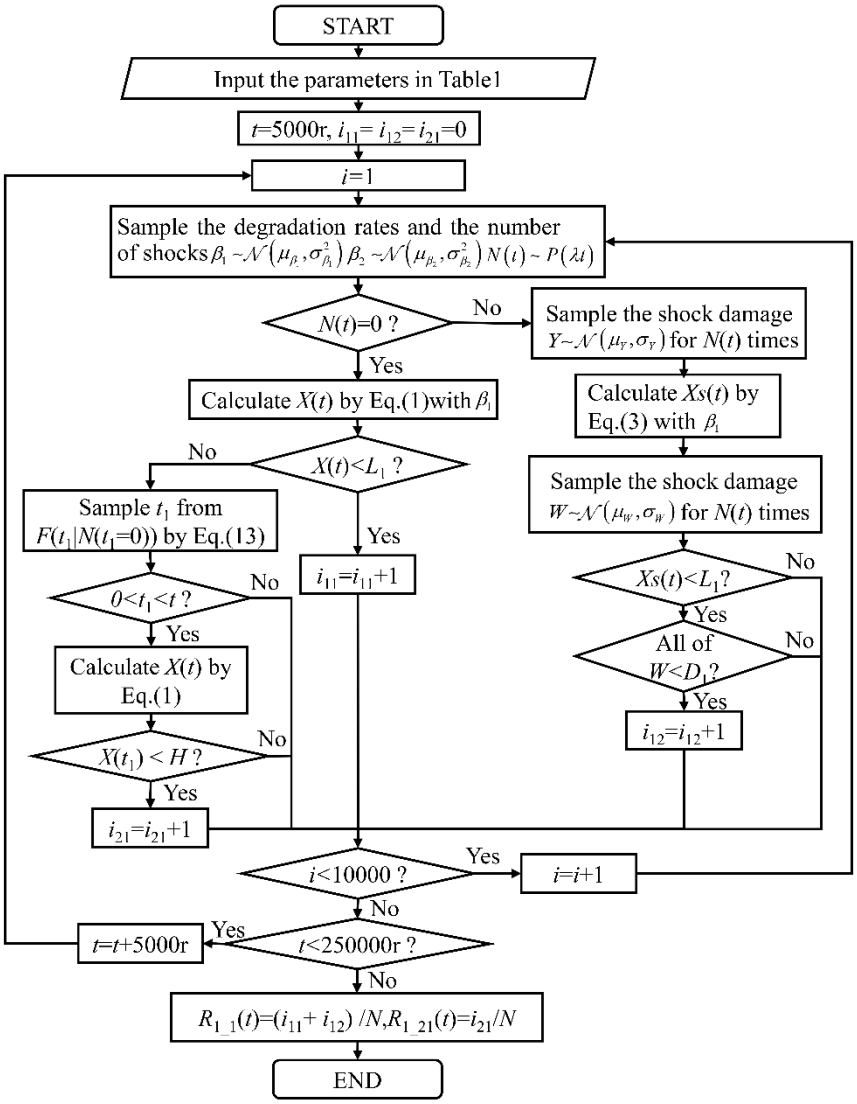

(a) The flow chart of the simulation procedure for $R_{1\_1}(t)$ and $R_{1\_21}(t)$

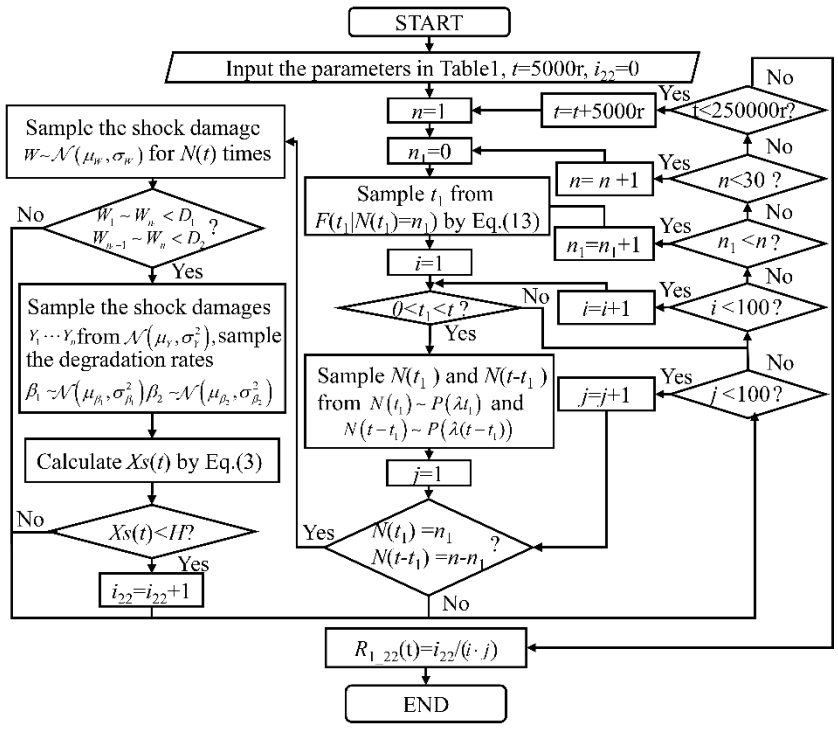

(b) The flow chart of the simulation procedure for $R_{1\_22}(t)$

Fig. C.1 Flow chart of the simulation for the system with k=1

References

[1] Huang XZ, Li YX, Zhang YM, Zhang XF. A new direct second-order reliability analysis method. Appl Math Model 2018; 55: 68-80. https://doi.org/10.1016/j.apm.2017.10.026.

[2] Sanchez-Silva M, Riascos-Ochoa J, Akhavan-Tabatabaei R. A review of challenges and strategies for modeling structural degradation. InStructures Congress 2014; 2257-2268.

[3] Zio E. Some challenges and opportunities in reliability engineering. IEEE Trans Reliab 2016; 65 (4): 1769-1782. https://doi.org/10.1109/TR.2016.2591504.

[4] Yousefi N, Coit DW, Song SL. Reliability analysis of systems considering clusters of dependent degrading components. Reliab Eng Syst Saf 2020; 202: 107005. https://doi.org/10.1016/j.ress.2020.107005.

[5] Li H, Pan DH, Chen CLP. Reliability modeling and life estimation using an expectation maximization based wiener degradation model for momentum wheels. IEEE T Cybern 2014; 45(5) : 969-977. https://doi.org/10.1109/TCYB.2014.2341113

[6] Lei J, Feng QM, Coit DW. Reliability and maintenance modeling for dependent competing failure processes with shifting failure thresholds. IEEE Trans Reliab 2012; 61(4): 932-948. https://doi.org/10.1109/TR.2012.2221016.

[7] Frangopol DM, Saydam D, Kim S. Maintenance, management, life-cycle design and performance of structures and infrastructures: a brief review. Struct Infrastruct E 2012; 8(1): 1-25. https://doi.org/10.1080/15732479.2011.628962

[8] Amaya-Gomez R, Riascos-Ochoa J, Munoz F, Bastidas-Arteaga E, Schoefs F, Sanchez-Silva M. Modeling of pipeline corrosion degradation mechanism with a Lévy Process based on ILI (In-Line) inspections. Int J Pres Ves and Pip 2019; 172:261-71. https://doi.org/10.1016/j.ijpvp.2019.03.001.

[9] Lee YJ, Song J, Gardoni P, Lim HW. Post-hazard flow capacity of bridge transportation network considering structural deterioration of bridges. Struct Infrastruct E 2011; 7(7-8): 509-521. https://doi.org/10.1080/15732479.2010.493338

[10] Gao HD, Cui LR, Kong DJ. Reliability analysis for a Wiener degradation process model under changing failure thresholds. Reliab Eng Syst Saf 2018; 171: 1-8. https://doi.org/10.1016/j.ress.2017.11.006.

[11] Peng WW, Li YF, Yang YJ, Zhu SP, Huang HZ. Bivariate analysis of incomplete degradation observations based on inverse Gaussian processes and copulas. IEEE Trans Reliab 2016; 65(2): 624-639. https://doi.org/10.1109/TR.2015.2513038.

[12] Cheng T, Pandey MD. An accurate analysis of maintenance cost of structures experiencing stochastic degradation. Struct Infrastruct E 2012; 8(4):329-39. https://doi.org/10.1080/15732479.2011.563088.

[13] Van Noortwijk JM, Van Der Weide JA, Kallen MJ, Pandey MD. Gamma processes and peaks-over-threshold distributions for time-dependent reliability. Reliab Eng Syst Saf 2007; 92(12):1651-1658. https://doi.org/10.1016/j.ress.2006.11.003

[14] Caballe NC, Castro IT, Pérez CJ, Lanza-Gutiérrez JM. A condition-based maintenance of a dependent degradation-threshold-shock model in a system with multiple degradation processes. Reliab Eng Syst Saf 2015; 134: 98-109. https://doi.org/10.1016/j.ress.2014.09.024.

[15] Liu B, Xie M, Xu ZG, Kuo W. An imperfect maintenance policy for mission-oriented systems

subject to degradation and external shocks. Comput Ind Eng 2016; 102: 21-32. https://doi.org/10.1016/j.cie.2016.10.008.

[16] Zhang J, Huang XY, Fang YT, Zhou J, Zhang H, Li J. Optimal inspection-based preventive maintenance policy for three-state mechanical components under competing failure modes. Reliab Eng Syst Saf 2016; 152: 95-103. https://doi.org/10.1016/j.ress.2016.02.007.

[17] Dong QL, Cui LR. A study on stochastic degradation process models under different types of failure thresholds. Reliab Eng Syst Saf 2019; 181: 202-212. https://doi.org/10.1016/j.ress.2018.10.002.

[18] Lei J, Feng QM, Coit DW. Modeling zoned shock effects on stochastic degradation in dependent failure processes. IIE Trans 2015; 47 (5): 460-470. https://doi.org/10.1080/0740817X.2014.955152.

[19] An ZW, Sun DM. Reliability modeling for systems subject to multiple dependent competing failure processes with shock loads above a certain level. Reliab Eng Syst Saf 2017; 157: 129-138. https://doi.org/10.1016/j.ress.2016.08.025.

[20] Fan MF, Zeng ZG, Zio E, Kang R. Modeling dependent competing failure processes with degradation-shock dependence. Reliab Eng Syst Saf 2017; 165: 422-430. https://doi.org/10.1016/j.ress.2017.05.004.

[21] Song SL, Coit DW, Feng QM. Reliability analysis of multiple-component series systems subject to hard and soft failures with dependent shock effects. IIE Trans 2016; 48(8): 720-735. https://doi.org/10.1080/0740817X.2016.1140922.

[22] Song SL, Coit DW, Feng QM, Hao P. Reliability analysis for multi-component systems subject to multiple dependent competing failure processes. IEEE Trans Reliab 2014; 63(1): 331-345. https://doi.org/10.1109/TR.2014.2299693.

[23] Liu HL, Yeh RH, Cai BP. Reliability modeling for dependent competing failure processes of damage self-healing systems. Comput Ind Eng 2017; 105: 55-62. https://doi.org/10.1016/j.cie.2016.12.035.

[24] Bian L, Gebraeel N. Stochastic Modeling and Real-Time Prognostics for Multi-Component Systems with Degradation Rate Interactions. IIE Trans 2014a; 46(5): 470-82. https://doi.org/10.1080/0740817X.2013.812269.

[25] Bian L, and Gebraeel N. Stochastic framework for partially degradation systems with continuous

component degradation-rate-interactions. Nav Res Log 2014; 61(4): 286-303. https://doi.org/10.1002/nav.21583.

[26] Dao CD, Zuo MJ. Selective maintenance for multistate series systems with s-dependent components. IEEE Trans Reliab 2015; 65(2): 525-539. https://doi.org/10.1109/TR.2015.2494689.

[27] Shen JY, Elwany A, Cui LR. Reliability analysis for multi-component systems with degradation interaction and categorized shocks. Appl Math Model 2018; 56: 487-500. https://doi.org/10.1016/j.apm.2017.12.001.

[28] Dong QL, Cui LR, Si SB. Reliability and availability analysis of stochastic degradation systems based on bivariate Wiener processes. Appl Math Model 2020; 79: 414-433. https://doi.org/10.1016/j.apm.2019.10.044.

[29] Hao SH, Yang J. Reliability analysis for dependent competing failure processes with changing degradation rate and hard failure threshold levels. Comput Ind Eng 2018; 118: 340-351. https://doi.org/10.1016/j.cie.2018.03.002.

[30] Rafiee K, Feng QM, Coit DW. Reliability modeling for dependent competing failure processes with changing degradation rate. IIE Trans 2014; 46(5): 483-496. https://doi.org/10.1080/0740817X.2013.812270.

[31] Gao HD, Cui LR, Qiu QG. Reliability modeling for degradation-shock dependence systems with multiple species of shocks. Reliab Eng Syst Saf 2019; 185: 133-143. https://doi.org/10.1016/j.ress.2018.12.011.

[32] Wang XG, Li L, Chang MX, Han KZ. Reliability modeling for competing failure processes with shifting failure thresholds under severe product working conditions. Appl Math Model 2020; 89: 1747-1763. https://doi.org/10.1016/j.apm.2020.08.032.

[33] Hao SH, Yang J, Ma XB, Zhao Y. Reliability modeling for mutually dependent competing failure processes due to degradation and random shocks. Appl Math Model 2017; 51: 232-249. https://doi.org/10.1016/j.apm.2017.06.014.

[34] Akiyama M, Frangopol DM, Matsuzaki H. Life-cycle reliability of RC bridge piers under seismic and airborne chloride hazards. Earthquake Engineering & Structural Dynamics 2011; 40(15): 1671-1687. https://doi.org/10.1002/eqe.1108

[35] Rafiee K, Feng QM, Coit DW. Reliability analysis and condition-based maintenance for failure processes with degradation-dependent hard failure threshold. Qual Reliab Eng Int 2017; 33 (7): 1351-1366. https://doi.org/10.1002/qre.2109.

[36] Guan XM, Zhao GY, Xuan J. Reliability modeling for multi-component systems subject to multiple dependent competing failure processes with shifting hard failure threshold. PHM-Harbin, IEEE 2017:1-7. https://doi.org/10.1109/PHM.2017.8079117.

[37] Sanchez-Silva M, Klutke GA. Degradation: Data Analysis and Analytical Modeling. In: Reliability and Life-Cycle Analysis of Deteriorating Systems 2016, p. 79-116. Springer; 2016, p. 79-116.

[38] Riascos-Ochoa J, Sanchez-Silva M, Klutke GA. Modeling and reliability analysis of systems subject to multiple sources of degradation based on Lévy processes. Probabilist Eng Mech 2016; 45: 164-76. https://doi.org/10.1016/j.probengmech.2016.05.002

[39] Jia G, Gardoni P. State-dependent stochastic models: A general stochastic framework for modeling deteriorating engineering systems considering multiple deterioration processes and their interactions. Struct Saf 2018; 72: 99-110. https://doi.org/10.1016/j.strusafe.2018.01.001

[40] Shailesh KR, Kurian CP, Kini SG. LED lighting reliability from a failure perspective. ICETEEEM, IEEE 2012: 468-472. https://doi.org/10.1109/ICETEEEM.2012.6494509.

[41] Yang B, Dai S, Liao Z, Meng F, Xiao SN, Yang GW, Zhu T. Influence of Tension-torsion Stress Amplitude Ratio on Short Fatigue Crack Behaviour of LZ50 steel. J Mech Eng 2020; 56(16): 33-43. https://doi.org/10.3901/JME.2020.16.033.

[42] Tanner DM, Miller WM, Peterson KA, Dugger MT, Eaton WP, Irwin LW, Senft DC, Smith NF, Tangyunyong P, Miller SL. Frequency dependence of the lifetime of a surface micromachined microengine driving a load. Microelectron Reliab 1999; 39(3): 401-414. https://doi.org/10.1016/S0026-2714(98)00248-0.

[43] Peng H, Feng QM, Coit DW. Simultaneous quality and reliability optimization for microengines subject to degradation. IEEE Trans Reliab 2009; 58(1): 98-105. https://doi.org/10.1109/TR.2008.2011672.